



Affinity biosensors developed with quantum dots in microfluidic systems

Sultan Şahin^{1,2,3} · Caner Ünlü^{1,2,4} · Levent Trabzon^{1,2,3,5} 

Received: 18 November 2020 / Accepted: 18 February 2021 / Published online: 10 March 2021
© Qatar University and Springer Nature Switzerland AG 2021

Abstract

Quantum dots (QDs) are synthetic semiconductor nanocrystals with unique optical and electronic properties due to their size (2–10 nm) such as high molar absorption coefficient (10–100 times higher than organic dyes), resistance to chemical degradation, and unique optoelectronic properties due to quantum confinement (high quantum yield, emission color change with size). Compared to organic fluorophores, the narrower emission band and wider absorption bands of QDs offer great advantages in cell imaging and biosensor applications. The optoelectronic features of QDs have prompted their intensive use in bioanalytical, biophysical, and biomedical research. As the nanomaterials have been integrated into microfluidic systems, microfluidic technology has accelerated the adaptation of nanomaterials to clinical evaluation together with the advantages such as being more economical, more reproducible, and more susceptible to modification and integration with other technologies. Microfluidic systems serve an important role by being a platform in which QDs are integrated for biosensing applications. As we combine the advantages of QDs and microfluidic technology for biosensing technology, QD-based biosensor integrated with microfluidic systems can be used as an advanced and versatile diagnostic technology in case of pandemic. Specifically, there is an urgent necessity to have reliable and fast detection systems for COVID-19 virus. In this review, affinity-based biosensing mechanisms which are developed with QDs are examined in the domain of microfluidic approach. The combination of microfluidic technology and QD-based affinity biosensors are presented with examples in order to develop a better technological framework of diagnostic for COVID-19 virus.

Keywords Quantum dots · Microfluidic systems · Biosensors

1 Introduction

Quantum dots (QDs) are semiconductor nanocrystals which show unique optical and electronic properties due to their size (2–10 nm). The size of QDs is smaller than the Bohr radius,

which quantizes energy levels and as a result, QDs exhibit very different optoelectronic properties from bulk materials due to quantum confinement effect. So far, QDs have been intensively used in important research areas such as bioimaging [1, 2], diagnostic [3], drug imaging [4], and biomolecular interactions [5–8].

Many of the organic dyes and protein-based fluorophores have serious chemical and photophysical problems such as photochemical changes, pH sensitivity, and short-term stabilization in aqueous medium. These problems restrict the effectiveness of organic fluorophores in cell imaging and biosensor applications. In general, fluorophores have narrow absorption and wide emission bands. However, the narrow emission bands and symmetrical bands in the wide absorption spectrum of QDs offer great advantages in cell imaging and biosensor applications compared to organic fluorophores. These features of QDs can be used to trace multiple biological targets simultaneously without need of complex instrumentation. To mention other advantageous properties of QDs, they have higher quantum

✉ Levent Trabzon
levent.trabzon@itu.edu.tr

¹ Nanoscience and Nanoengineering Department, Istanbul Technical University, Istanbul, Turkey

² Nanotechnology Research and Application Center – ITUNano, Istanbul Technical University, Istanbul, Turkey

³ MEMS Research Center, Istanbul Technical University, Istanbul, Turkey

⁴ Department of Chemistry, Istanbul Technical University, Istanbul, Turkey

⁵ Faculty of Mechanical Engineering, Istanbul Technical University, Istanbul, Turkey

efficiency as well as the higher molar absorption coefficient (10–100 times) compared to organic dyes and have wider Stokes shifts. QDs also offer some advantages in electrochemical applications with their semiconductor features; electrochemical luminescence (ECL) emission ability, effective redox ability, and low power requirements in applications [9, 10]. All these superior physical and chemical features of QDs have led to their intensive use in bioanalytical, biophysical, and biomedical research [11–13].

Another important research field benefiting from the optoelectronic and electrochemical advantages of QDs is biosensor applications. In recent biosensor studies, trend toward using QDs instead of the fluorophores is increasing. QDs are preferred to develop both optical and electrochemical transduction systems in affinity [14–16] and catalytic [17–19] biosensor applications. Integration of a biosensing mechanism in the microfluidic system brings an innovative approach to biosensor applications. Design of microfluidic systems and different microfabrication methods enhance biosensor performance and comfort of use by increasing sensitivity, decreasing response time, multiplexed detection, being portable, miniaturizable, small amount sample requirement, and being allowed integration multiple transduction systems.

The technology of microfluidic would make it possible to accelerate the use of nanoparticles in clinical evaluation with its advantages of being economical, reproducible, and susceptible to modification and integration with other technologies [20, 21]. Microfluidic systems are the evaluation of microfluidic disciplines and microsystems based on the use and/or transfer of fluids in various mechanisms in devices with an inner size of μm range [22, 23]. This obtains controlled diffusion within the microsystem, stable, and homogeneous liquid–liquid interface interactions in cellular dimensions. A combination of integrated microfluidics systems has also revealed the field of “Micro Total Analysis Systems (μTAS)”, in different words “On-Chip Laboratory (Lab-on-Chip-LoC) technology [24, 25]. By using advanced microfabrication techniques with LoC technology, protocols that can be realized in macro-scale laboratory conditions are used in micro-scale by using microfluidic channels, micro-mixers, micro-heaters, micro-valves, and micro-pumps together on the chip [26]. Thus, the development of portable, automatic, and fast-responsive devices has become possible with the improvement of LoC technologies in recent years. The downsizing of devices also reduces the use of fewer ingredients for an experimental procedure that can be developed in the chip and also contributes to a homogeneous and standard synthesis formation. The desired processes have been developed by designing microchannels suitable for the electrodes and patterned surfaces, modifying them in various applications, and with various nanomaterials [20].

Thus, it is an advisable approach to combine the advantages of QDs with microfluidic system technology in order to obtain unique and versatile platform in biosensor applications.

Mass transfer in short diffusion distance in the microfluidic system and the large surface area/volume ratio of the QDs enable to reduce response time of the optical sensor and increase sensitivity of sensor [27]. In this perspective, there are some very recent attempts for Covid-19 detection, such as developing affinity-based optical biosensors with QDs in a lateral flow immunoassay to detect IgG/IgM which are specific for SARS CoV-2 [28, 29]. In this review, considering all the advantages of QDs and microfluidic systems, we present a holistic perspective by reporting the related studies on the use of QDs with microfluidic systems and affinity biosensors. Thus, a new approach would be established in order to develop the point-of-care (PoC) field for diagnostic in pandemic times.

For the sake of completeness, we will explain important features of bioelements in biosensing in the first section, and then the use of QDs in microfluidic system is discussed in terms of affinity sensing with a focus of optical and electrochemical approaches in the second part, and design and fabrication issues of QD-based affinity sensors will be given in the last section. Moreover, the use of microfluidic system with QDs to diagnose COVID-19 will also be elaborated in the corresponding sections with a future perspective at the end.

2 Affinity biosensors

A biosensor is an analytical detection device that converts physicochemical changes on its transducer part to quantifiable signal by electronic parts of it. The transducer part of biosensors is modified by bioelements that interact with an analyte which is desired to be detected, wherein the result of this interaction appears as a physicochemical change like electrical, optical, mass, or thermal change. In terms of affinity biosensors incorporating affinity-based bioelements which are immobilized on or near the transducer, bioelements can reversibly detect analytes with a high selectivity and affinity nondestructively [30, 31]. The principle of affinity biosensors is a stable and selective formation between an appropriate analyte–bioreceptor which gives a response signal by a transducer. Bioelements that are incorporated in affinity biosensors are commonly antibody–antigen, oligonucleotides, aptamers, and molecularly imprinted polymers. Phages, molecularly imprinted polymers (MIPs), aptamers, and peptide nucleic acids (PNAs) are used as new generation of affinity bioelements. These receptor molecules are used in various types of transducers to analyze the interaction; such as quartz crystal microbalance (QCM), surface plasmon resonance (SPR), surface acoustic wave, fluorescence spectroscopy, total internal reflection fluorescence, amperometry, potentiometry, and impedance spectroscopy [32]. Bioelements, which are commonly used in biosensing, will be briefly introduced in the coming sections.

2.1 Antibody–antigen interaction-based biosensors

Antibodies are proteins that are produced in response to foreign substances (antigens), such as toxins, drugs, virus particles, and bacterial toxins. Production of antibodies is based on animal immunization by white blood cells against the antigen. Limitations of using antibodies due to their protein structure are pH, temperature sensitivity, short shelf life, and easy degradation. They can be integrated with a variety of biosensor applications at appropriate conditions. Biosensors developed by antibody–antigen interaction are called immunosensors and various transduction methods have been used in immunosensor studies such as optical, electrochemical, mass-based transduction. Commercially available and most frequently used immunoassays are enzyme-linked immunosorbent assay (ELISA), radioimmunoassay, and chemiluminescent immunoassay [33, 34].

2.2 Nucleic acid-based biosensors

The principle of the nucleic acid-based biosensors lies in hybridization between complementary and template single-stranded deoxyribonucleic acid (ssDNA) or ribonucleic acid (ssRNA). Due to the hybridization characteristics of oligonucleotide probes, they are immobilized on a transduction platform to be hybridized with the target sequence. Other nucleic acids are PNAs which are synthetic oligonucleotide analogs that exhibit superior hybridization characteristics and improved chemical (wide range of temperatures and pHs) and enzymatic stability, therefore making them more feasible than DNA [35]. Since more durable and stable biosensors are developed with artificially synthesized PNA sequences, various transduction methods have been integrated with PNA in affinity sensors [36, 37].

2.3 Aptamer-based affinity biosensors

Aptamers are either ssDNA or RNA and peptide molecules that are capable of binding to a wide range of target proteins with high affinities and specificities. Aptamers show exponential expansion with significant advantages for affinity biosensing applications. They undergo a significant conformational change in the three-dimensional structure and folding pattern upon binding to the target. As an alternative to natural antibodies, aptamers possess high affinity and specificity. Aptamers can be easily modified with a variety of functionalities such as fluorescent labels, biotin, and enzymes; it makes possible to have the design of flexible sensing platforms in addition to some advantages which are less expensive, more stable, and easy synthesis [38].

2.4 Molecularly imprinted polymer-based biosensors

MIPs are described as plastic antibodies, because of their selectivity against an analyte. Polymerization around the template molecule is attributed to the process of “molecular imprinting”. After molecular imprinting process, template molecules are rinsed from polymer structure to obtain a well-defined complementary cavity to template molecule on the surface of the polymer structure. The advantages of MIPs involve their high chemical and physical stability in that they hardly decompose or they demand no specific storage conditions. Therefore, in affinity biosensor applications, MIPs are preferred increasingly [39]. There are also some drawbacks of MIPs; such as, leakage or incomplete removal of the template, random distribution of binding site, nonhomogenous morphology, and slow mass transfer [40].

3 Integration of an affinity biosensor by quantum dots in microfluidic system

In an affinity biosensor construction by QDs in microfluidic system, conjugation between QDs and bioelement is a very critical step. The conjugation of QDs with biomolecules began by creating a fluorescent label for biological imaging in the early 1990s [41]. Covalent or non-covalent binding approaches are used for conjugation of biomolecule-QDs. Accepted and frequently applied QD conjugation protocols in bioapplications are streptavidin/avidin binding to biotin, carbodiimide chemistry (EDC/NHS binding), and maleimide thiol binding [42]. In EDC/NHS (1-Ethyl-3-(3-dimethylaminopropyl)carbodiimide/N-hydroxysuccinimide) chemistry; EDC binding to the NHS carboxyl group forms an amide bond between QDs and protein by creating an intermediate of O-acylurea that replaces first-degree amines. Amine-bound QDs can also be biotinylated using the NHS molecule and then they can be easily conjugated with streptavidin-bound biomolecules. Controlling the orientation and the number of biomolecules bound on the QD is crucial in order not to affect the active binding site (affinity) of the biomolecule [11, 42, 43]. Response mechanisms of conjugated QDs for an affinity-based interaction are Förster resonance energy transfer (FRET), bioluminescence resonance energy transfer (BRET), charge transfer (CT), quenching, and electrochemical luminescence [43]. In affinity biosensors, different types of nanoparticles have been used as labels to enhance the sensitivity of optical and electrochemical assays. Among these nanoparticles, QDs have been widely used to develop effective optical and electrochemical biosensing. Sensitivity and reliability were also increased in the detections with the use of QD-conjugated bioelements.

It is exemplified by QD-based affinity to show increased sensitivity of biosensor. Carcinoma embryonic antigen (CEA)

and α -fetoprotein (AFP) cancer biomarkers are bound to CdSe QDs by EDC/NHS chemistry and biomarkers are measured providing a detection linear range of 0.5–500 ng/mL with fluorescence emission after affinity-based interaction. Compared with the commercial ELISA kit, high compliance was detected in the QD-conjugated system with serum samples and 97.0–107.4% recovery in CEA detection, 93.0–104% recovery in AFP detection was handled [16]. Detection of Zika virus antibodies was studied by fluoroimmunological measurement with QDs in 2019 [44]. In this study, interaction with Zika virus antibodies was implemented on polystyrene microplate coated with Zika virus E proteins. Zika virus antibodies were detected by fluorescence intensity obtained with secondary antibodies conjugated with QDs. In the ELISA system, enzymes are conjugated to secondary antibodies, when the secondary antibody binds to the target molecule, it differs in enzymatic activity and the color change is observed on the microplate. However, QDs were used instead of enzymes in this system to detect Zika virus antibodies and higher sensitivity was obtained compared to ELISA tests.

The emission of QDs in different sizes at different wavelengths in narrow ranges is used to detect multiple target molecules which is also defined as QD barcoding in the literature. H9 avian influenza virus and MHV68 virus were independently determined qualitatively with CdTe QDs that emit green fluorescence light at 535 nm emission wavelength and orange fluorescence light at 585 nm emission wavelength [45]. This sensitive sensing mechanism needs a suitable platform to be useful in applicable platforms. Microfluidic systems can be used as a platform to get highly sensitive QD integrated affinity biosensor in a virus detection with high correctness.

Development of an affinity biosensor in microfluidic system is very convenient for designs and diversity of integration. In recent years, microdevices have been developed to detect smaller pathogens like coronavirus, the human immunodeficiency virus (HIV), and Zika virus [46, 47]. Recently, SARS CoV-2 polymerase chain reaction (PCR) was performed in electrochemical microfluidic device with detection of amplified nucleic acids on a Silicon-based transducer [48]. In another study, an optical microfluidic device was developed to detect antibodies against SARS CoV-2 (Covid-19) by localized surface plasmon resonance transduction method. Antibodies against the SARS-CoV-2 spike protein were detected in approximately 30 min in a diluted human plasma (1:1000), with the limit of detection (LOD) of 0.08 ng/mL [49]. Fluorescence-Based multiple detection system for IgG, IgM antibodies and antigen of SARS-CoV-2 were developed simultaneously in a single microfluidics chip within 15 min [50]. In general aspect, microfluidic devices also offer multiple advantages such as detection in a shorter duration, low cost, capacity of multiplexing, no sample pretreatment, as

well as the system can be integrated with other platforms to induce higher specificity, sensitivity, and selectivity [51–53] so that a versatile approach is to be developed to diagnose pathogenic organisms including Covid-19.

To obtain a comprehensive approach for integration of QD-conjugated biosensing mechanisms and microfluidic system to construct an affinity biosensor, optical and electrochemical transduction methods are also specifically reviewed and exemplified with related findings in Sections 3.1 and 3.2. Specifically, optical and electrochemical affinity biosensors with QDs in the microfluidic system research of the last two decades are reviewed in Table 1. In these studies, active sensing regions were created in the microfluidic system, where optoelectronic changes occur as a result of the interaction of the target molecule and QD-conjugated bioelement.

3.1 Optical affinity biosensors by quantum dots in microfluidic system

In affinity-based biosensor studies with QDs, it has been shown that a more sensitive and reliable detection can be made. Conjugation of QDs with biomolecules has been experimented for protein detection in applications such as ELISA [75], Western blotting [76], and microarray [77]. Small organic dye molecules are commonly preferred in such systems. Considering the advantages of QDs, studies have been carried out to use QDs in the most efficient way instead of fluorescent dyes. The aforementioned features of QDs make an optical detection more sensitive, reliable, and give the ability to make multiple optical detections at the same time. QDs modified with biomolecules are generally used in solution or by binding on a solid phase such as microsphere. Steric hindrance of modified QDs in the solution has created a trend that it will be more advantageous to use it by depositing it on a certain support surface. On the other hand, there is a challenging problem of colloidal stability in the solution, but microfluidic systems designed with microfabrication techniques create a suitable platform to maintain its stability [20, 27, 57]. When microfluidic system technology is combined with the advantages of QDs, biosensors capable of optical detection would be better in quality.

In the study about the development of a lateral flow test, two different subtypes of Influenza A (H5 and H9) were detected at the same time by conjugating antibodies with QDs [78]. The test strips were developed with the sandwich-type immunological detection principle and integrated into a small portable device (fluorescent scanner). The fluorescence emission intensity results from interactions between antigen–antibody were detected in 15 min with the fluorescent scanner. After H5, H9, and control lines were stimulated with UV at 365 nm wavelength, QD-conjugated antibodies produced a bright fluorescent emission in affinity lines. The limit of detection (LOD) was determined as 0.016 HAU (hemagglutinated unit) and 0.25

Table 1 Affinity biosensors by quantum dots in microfluidic systems

Binding chemistry, bioelement immobilization, deposition	Quantum dots	Target	Fluid flow driven Flow rate	Microchannel dimensions/material	Output	Year ^{Ref}
Optical affinity biosensors by quantum dots in microfluidic systems						
QD-anti human IgG: commercial	Anti-human IgG-conjugated CdSe/ZnS QD ₅₆₅	Anti-human IgG	Syringe pump	Microwell: 50 μm × 50 μm × 30 μm	<ul style="list-style-type: none"> Polystyrene microbead-based optical immunoassay Multifunctional microwell plate capturing of bio-materials into multiple microwells, well isolation, and the introduction of specific chemicals A single microbead captured and isolated inside a designated microchamber in a small volume of 75 pL 	2006 [54]
QD-antigen:carbodiimide chemistry (EDC/NHS coupling)	CdSe/ZnS QD ₅₇₀ and 615	HBsAg, NSP ₄ , and gp41	Electrokinetically	100 μm wide 15 μm high (PDMS)	<ul style="list-style-type: none"> LOD: 0.1 μg/mL Multiplex detection by QD barcodes 50-fold improvement in sensitivity compared ELISA kits for anti-HBsAg and anti-gp41 (10⁻¹⁰–10⁻¹² M) 	2007 [55]
QD-antibodies (IgG): SMCC/DTT	CdSe/ZnS QD ₅₆₅ and 655	CEA, CA125, and Her-2/Neu (CerbB-2)	Peristaltic pump 0.2–1.1 mL/min	(PMMA)	<ul style="list-style-type: none"> Multiplex detection Response time: 27 min Linear detection range: 0–100 ng/mL CEA, 0–60 ng/mL Her-2/Neu, and 0–400 U/mL CA125 LODs: 0.02 ng/mL CEA, 0.27 ng/mL Her-2/Neu Selective and reproducible 	2009 [56]
QD-IgG:carbodiimide chemistry (EDC/NHS coupling)	CdTe/CdS QD ₅₃₀ , 564, and 595	CEA and AFP	Syringe pump	150 μm wide 30 μm high (PDMS)	<ul style="list-style-type: none"> Multiplex detection High brightness than Cy3-IgG Detection linear range: 25 fM to 25 nM LOD of CEA and AFP is 250 fM 	2010 [57]
Immobilization:van der Waals interactions between antibody and PDMS, blocking reagent is BSA					Real sample analysis is successful	
QD-streptavidin-oligonucleotides: Avidin-Streptavidin	QD ₅₆₅ streptavidin conjugate	Oligonucleotides for B, C, D, E HBV DNA	Syringe pump	Microwell: 150 μm × 200 μm × 30 μm (w-l-d) Microchannel: 500 μm × 2 mm × 10 μm (w-l-d) (PDMS)	<ul style="list-style-type: none"> Multiplex detection for 4 different genotypes of HBV 1 × 10³ copies/mL of HBV virus could be detected and identified its genotypes LOD: 4 pM Reaction time: <30 min 	2010 [58]
QD-oligonucleotide: MPA/thiol modified oligonucleotide	CdSe/ZnS QD ₅₂₄	Oligonucleotide	Electrokinetically	250 μm wide 9 μm depth (PDMS)	<ul style="list-style-type: none"> FRET based optical detection in microfluidic channel Sample volume: 1 μL Detection time: 5 min 	2011 [59]
QD-BSA-2,4-D: EDC/Sulfo NHS chemistry	Carboxyl coated CdSe/ZnSe QD ₆₀₅	2,4-D	Syringe pump	600 μm × 100 μm (glass)	<ul style="list-style-type: none"> High-efficiency FRET and high sensitivity Linear detection range: 0.5 μM to 30 μM LOD: 0.5 nM S/N: 3 Response time: 6 min 	2012 [60]
QD-streptavidin: commercial		Adenosine and cocaine	NA	100 μm × 100 μm × 30 μm	<ul style="list-style-type: none"> Multiplex detection by bead based array 	2014 [61]

Table 1 (continued)

Binding chemistry, bioelement immobilization, deposition	Quantum dots	Target	Fluid flow driven Flow rate	Microchannel dimensions/material	Output	Year ^{Ref}
QD-anti-Salmonella antibodies: SMCC/DTT	Streptavidin-co-njugated CdSe/ZnS QD ₆₀₅	<i>S. typhimurium</i> bacterial cells	Peristaltic pump 40 µL/min	(w × l × d)-microchamber 150 µm × 1500 µm × 10 µm (w × l × d)-microchamber (PDMS)	<ul style="list-style-type: none"> Linear detection range for adenosine: 0.5–50pM for cocaine: 1–100pM Based on the dual signal amplification strategy LODs: 0.1pM and 0.5 pM for adenosine and cocaine Sample volume: 10 µL <i>S. typhimurium</i> concentration of 10³ CFU/mL in the borate buffer sample gave positive result within 30min Linear detection range: 0–10⁶ CFU/mL in real (R²= 0.949) and artificial (R²=0.995) samples LOD: 10³ CFU/mL <i>S. typhimurium</i> in real sample 	2015 [62]
MSN/QD-aptamer: MSN-CTAB-APTES/QD-EDC-NHS/DNA Aptamer	CdTe QD ₅₃₃₋₅₆₆	MCF-7, HL-60, and K562 cells	Capillary action	Paper based microchannels	<ul style="list-style-type: none"> Selective for Salmonella bacteria Multiplex detection Paper-based analytical device was developed (Cheap and easy usable) Linear detection range: 180 to 8 × 10⁷, 210 to 7 × 10⁷, 200 to 7 × 10⁷ cells/mL for MCF-7, HL-60, and K562 cells, respectively LODs: 62, 70 and 65 cells/mL Highly selective Linear detection range: 200–2000 ng/mL R²=0.9677 LOD: 56 ng/mL Response time: 10 min Selective for Ara h1 	2016 [63]
QD-aptamer: biotin/streptavidin	Streptavidin-co-njugated CdSe QD ₅₄₅	Ara h1	Capillary pump	200 µm width 60 µm height (PDMS)	<ul style="list-style-type: none"> Paper-based analytical device was developed (cheap and easy usable) Linear detection range: 10–50 mg/L R²=0.988 LOD: 2 mg/L Response time: 25 min Reproducibility RSD: 4.7% Storage stability: Over 7 days 94.3–105.7% recovery (RSD: 3.6–5.7%) for sea water 93.1–106.7% recovery (RSD: 3.3–5.1%) for lake water 	2016 [64]
Cellulose paper-QD: APTES/EDC/NHS	CdTe QD ₅₄₅₋₅₆₀	Phycocyanin	Capillary action	Paper based microchannels	<ul style="list-style-type: none"> Paper-based analytical device was developed (cheap and easy usable) Linear detection range: 10–50 mg/L R²=0.988 LOD: 2 mg/L Response time: 25 min Reproducibility RSD: 4.7% Storage stability: Over 7 days 94.3–105.7% recovery (RSD: 3.6–5.7%) for sea water 93.1–106.7% recovery (RSD: 3.3–5.1%) for lake water 	2017 [65]
QD@mSiO ₂ -anti CEA and anti AFP: carbodiimide chemistry (EDC/NHS coupling)	CdSe/ZnS QD _{550 and 590}	CEA and AFP	Syringe pump	High aspect ratio (thin channels) Breadth: 0.02 cm Thickness: 0.01 cm	<ul style="list-style-type: none"> Multiplex detection Linear range of CEA and AFP detections are 1.8 pg/mL–1.8 ng/mL and 0.68 pg/mL to 0.68 ng/mL More sensitive than ELISA kits LODs of CEA and AFP are 0.6 and 0.2 pg/mL 	2019 [15]

Table 1 (continued)

Binding chemistry, bioelement immobilization, deposition	Quantum dots	Target	Fluid flow driven Flow rate	Microchannel dimensions/material	Output	Year ^{Ref}
QD-Ab: EDC/NHS	CdTe QD ₅₂₅ and 605	CEA and PSA	Capillary action	Paper based microchannels	<ul style="list-style-type: none"> • Multiplex detection at same detection zone • Paper based analytical device was developed (Cheap and easy usable) • Linear detection range: 1.0–40 ng/mL for both biomarkers • LODs: • Recovery for serum sample: 95–105% • Linear detection range: 1.0×10^2 to 1.0×10^7 CFU/mL • LOD: 43 CFU/mL • Mean recovery for <i>Salmonella</i> in spiked chicken meats: 99.7% • Selective 	2019 [66]
MnO ₂ -QD: NH ₂ -MnO ₂ by APTES /COOH-QD by EDC/NHSS	CdSe/ZnS QD ₆₅₁	<i>Salmonella</i> Typhimurium	Syringe pump 25 µL/min	400 µm height 2 mm length for mixing and incubation channel 11 mm length 3 mm width 1 mm height for separation chamber (PDMS)	<ul style="list-style-type: none"> • Recovery for serum sample: 95–105% • Linear detection range: 1.0×10^2 to 1.0×10^7 CFU/mL • LOD: 43 CFU/mL • Mean recovery for <i>Salmonella</i> in spiked chicken meats: 99.7% • Selective 	2020 [67]
MnO ₂ -QD-pAb: MnO ₂ -QD/EDC/BSA/pAb						
QD-MIP: TGA-QD/EDC-NHS-APTES-glass fiber	ZnSe QD _{370–400}	Cd ²⁺ and Pb ²⁺ ions	Capillary action	Paper-based microchannels	<ul style="list-style-type: none"> • Paper-based analytical device was developed (cheap and easy usable) • Linear detection range: 1 to 70 µg/L for Cd²⁺, 1 to 60 µg/L for Pb²⁺ R²=0.996, 0.993, respectively • LODs: 0.245 µg/L for Cd²⁺, 0.335 µg/L for Pb²⁺ • Sample volume: 30 µL • Selective • Recovery of sea water and lake water: 95.0%–105.1%, RSDs: 3.1%–5.6% 	2020 [68]
Electrochemical affinity biosensors by quantum dots in microfluidic systems						
QD-secondary Ab: EDC/NHS	CdTe and ZnSe QDs	cTnI and CRP	Syringe pump	(PDMS-GNP composite)	<ul style="list-style-type: none"> • Linear detection range: 0.01 to 50 µg/L for cTnI, 0.10 to 1.0 µg/L for CRP • LODs: 0.004 µg/L for cTnI, 0.22 µg/L for CRP • Sensitive 	2010 [14]
QD-MIP: EDC-NHS-QD/AIBN-AM-EDGMA	CdTe QD (Light red emission)	S-fenvalerate	Capillary action	Paper-based microchannels	<ul style="list-style-type: none"> • Linear detection range: 10^{-8} to 10^{-6} mol/L • LOD: 3.5×10^{-9} mol/L • Sample volume: 10 µL • Selective, sensitive 	2013 [69]
Streptavidin-conjugated QD: Commercial	CdSe/ZnS QD ₅₈₅	ApoE and hlgG	Syringe pump Flow rate: 5 µL/min	500 µm wide 50 µm depth 3 cm long (PDMS)	<ul style="list-style-type: none"> • Linear detection range: 10 to 100 ng/mL for hlgG, 10 to 200 ng/mL for ApoE • LODs: 1.72 ng/mL for hlgG, 12.5 ng/mL for ApoE 	2014 [70]
LB deposition of QD on ITO surface: TOPO capped CdSe QDs	CdSe QD	CML specific oligonucleotide sequences	Syringe pump Flow rate: 0.1–1.4 µL/min	ITO coated (thickness=150 Å) glass substrate PDMS microchannels: 200 µm/200 µm/2cm (width/height/length)	<ul style="list-style-type: none"> • Linear detection range: 1.0 µM–1 fM • At 1.0 µL/min flow rate, the response time of the microfluidics electrode is 60 s • It retains 90% of its response after 30 days of storage 	2015 [71]
Streptavidin-conjugated QD: commercial	CdSe/ZnS QD ₆₅₅	hlgG	Syringe pump			2016 [72]

Table 1 (continued)

Binding chemistry, bioelement immobilization, deposition	Quantum dots	Target	Fluid flow driven Flow rate	Microchannel dimensions/material	Output	Year ^{Ref}
GQD immobilization on silanized alumina nonoporous membrane: GQD-glutaraldehyde-Ab	GQD	Enrofloxacin and ampicillin	Flow rate: 5 $\mu\text{L}/\text{min}$ Syringe pump Flow rate: 5 $\mu\text{L}/\text{min}$	500 μm diameter and 50 μm thickness (PDMS) 2 chamber was divided by a nanoporous membrane (PDMS)	<ul style="list-style-type: none"> •100-fold better in microflow (sensitivity: 20×10^{-6} A/nM) than in batch mode (sensitivity: 0.2×10^{-6} A/nM) •Response time: 6.6 min •LOD: 3.5 ng/mL RSD: 13.2% •A new method for bacteria response to antibiotics investigation •Detection time: 30 min •Linear detection range: 1 nM to 100 pM for both targets •LODs: 1 pM for enrofloxacin, 40 pM for ampicillin 	2017 [73]
QD-oligonucleotide: avidin/streptavidin-conjugated QDs	Streptavidin-co-njugated CdSe/ZnS QD ₅₈₅	Oligonucleotide	Capillary action	Paper-based microchannels: 135 $\mu\text{m}/1.3$ cm	<ul style="list-style-type: none"> •Paper-based analytical device was developed (cheap and easy usable) •Linear detection range: 0.50 pmol/L to 50 nmol/L $R^2=0.993$ (n=5) •LOD: 0.11 pmol/L •Reproducibility of fabrication: 4.8%, DNA bioassay: 10.1–13.2% (% RSD) •Selective 	2018 [74]

Abbreviations: QD_x: Emission wavelength at x nm, EDC: 1-Ethyl-3-(3-dimethylaminopropyl)carbodiimide, NHS: N-hydroxysuccinimide, HBsAg: Hepatitis B surface antigen, HCV: Hepatitis C virus, NSP₄: HCV nonstructural protein 4, HIV: Human immunodeficiency virus, gp41: HIV glycoprotein 41, IgG: Immunoglobulin G, BSA: Bovine serum albumin, CEA: Carcinoembryonic antigen, AFP: α -fetoprotein, LOD: Limit of detection, Cy3: Cyanine, RSD: relative standard deviation, PSA: Prostate specific antigen, CA125: Carcinoembryonic antigen 125, PDMS: Polydimethylsiloxane, mSiO₂: mesoporous SiO₂, 2,4-D: 2,4-Dichlorophenoxyacetic acid, SMCC: Succinimidyl 4-[N-maleimidomethyl]cyclohexane-1-carboxylate, DTT: Dithiothreitol, LB: Langmuir–Blodgett, ITO: Indium thin oxide, CML: Chronic myelogenous leukemia, TOPO: Trioctylphosphine oxide, AF488: Alexa Fluor 488, MIP: Molecularly imprinted polymer, NA: Not available, ConA: Concanavalin A, MPA: 3-Mercaptopropionic acid, pAb: polyclonal Ab, NHSS: N-Hydroxysulfosuccinimide sodium, MSN: Mesoporous silica nanoparticles, CTAB: (1-hexadecyl)trimethylammoniumbromide, TGA: thioglycolic acid, ApoE: ApolipoproteinE, hIgG: Human IgG, QGD: Graphene QD, cTnI: Cardiac troponin I, CRP: C-reactive protein, HPI: Hairpin probe1, GNP: Gold nanoparticle, APTES: (3-Aminopropyl) triethoxysilane

HAU for H5 and H9, respectively, and matched 100% in positive/negative results compared to real-time PCR.

Parallel assays are possible in the QD-based biosensor with a microfluidic system. There is a good example for a parallel assay in a microfluidic system by QDs [58]. The QD-based optical biosensor was developed in a microfluidic system that can detect different genotypes of the hepatitis B virus (HBV). Biotinylated oligonucleotides were synthesized for HBV genotypes B, C, D, and E then they have been bound to avidin-functionalized microsphere. Separate sensing chambers were designed in the microfluidic system for 4 different genotypes immobilized to the microspheres and these microspheres were sent to the microchambers. By using QDs as a fluorescent label, the detection limit in the detection of the synthetic target ssDNA chain has been reduced to 4 pM. HIV (10^3 /mL copy) was detected in the microfluidic system that can separate the different HIV genotypes after RNA amplification from the serum and labeling it by QD. This study shows that multiple detections are possible not only with QDs emitting different wavelengths but also with microfluidic system design.

Three different cancer biomarkers were detected using QDs in a microfluidic system [56]. Linear detection ranges of Nano-bio-chip (NBC) system were 0–100 ng/mL, 0–60 ng/mL, and 0–400 U/mL for CEA, Her-2/Neu, and CA125, respectively. Compared to the QD-based sandwich assay and ELISA, the results were 1.9 times more sensitive. In the study, a performance comparison was also made with QD and fluorophore (Alexa Fluor 488-AF488) in the microfluidic system. LODs were measured for CEA with results of 0.02, 2.61, and 1.20 ng/mL for NBC-QD, NBC-AF488, and ELISA, respectively. LODs were measured for Her-2/Neu with results of 0.27, 3.70, and 1.50 ng/mL for NBC-QD, NBC-AF488, and ELISA, respectively. The sandwich assay developed with QDs has been shown to give better results for the detection of target molecules at very low levels.

A bead-based array was developed that can detect adenosine and cocaine in parallel in the microfluidic system [61]. Microbeads were functionalized with HRP (horseradish peroxidase) and aptamers specific to adenosine and cocaine, modified electron rich proteins, and streptavidin-conjugated QDs, gold nanoparticles (AuNPs). This multi-functional design provides a signal in dual amplification. Electron rich protein structure is constructed with casein modified by covalently coupling with 4-OH-PPA-NHS (3-(4-Hydroxyphenyl) propionic acid N-hydroxysuccinimide ester). The 3'-biotin modified aptamers and biotinylated 4-OH-PPA-casein conjugates were bonded to polystyrene beads. Microparticles functionalized with different aptamers were entrapped in different microchambers. Then, HRP solution with AuNPs as capture probe was passed over beads in order to induce hybridization with aptamer. After the washing steps, biotin-conjugated tyramine and peroxidase enzyme substrate, H_2O_2 , were sent in microflow. In the last step, streptavidin-QD conjugate was

sent for labeling and the fluorescence intensity was checked with a fluorescence microscope. A catalytic reaction was carried out in peroxidase substrate solution and a reporting step was followed using the streptavidin-conjugated QDs.

As stated in the examples, QDs are generally used as labeling agents in optical-based biosensors. In order to observe the interaction of QD-labeled biomolecules with the target molecule in the microsystem, it was necessary to create a detection zone. In some studies [62, 67], biomolecules and target molecules are attached to magnetic particles that are held in a certain place with a magnet by using superparamagnetic particles in immunomagnetic separation technique. Magnetic particles are entrapped in the detection zone by an externally applied magnetic field in the microfluidic system. The target cells were interacted with antibody-conjugated QDs, and antibody-bound superparamagnetic particles have flowed through two different inlets of the microsystem [62]. A borate buffer was used to drain unbound QDs. *Salmonella typhimurium* bacteria species optically were detected by magnetic separation in the microfluidic system with the results of 1.0×10^2 to 1.0×10^7 for CFU/mL and LOD 43 CFU/mL for LOD [67]. QD-MnO₂-pAb complex was sent from the 1st inlet of the microchannel, and the target molecule *Salmonella typhimurium* bacteria cells and modified magnetic nanoparticles (MNPs) by Anti *Salmonella typhimurium* monoclonal Ab (mAb) were sent through the 2nd inlet of the microfluidic system for mixing and incubation. Then, the complex structure of QD-MnO₂-pAb-MNP-mAb-*Salmonella typhimurium* was kept in the detection zone by externally applied magnetic field. The optical detection was achieved by using glutathione (GSH) solution at the 3rd inlet. Thus, with the fluorescence intensity determined by the releasing of QDs from QD-MnO₂-pAb-MNP-mAb-*Salmonella typhimurium* complex, the amount of *Salmonella typhimurium* bacteria was correlated with the intensity of measurement.

In addition to developing biosensors by observing the fluorescence change after the interaction of the target molecules with QD-labeled biomolecules in the microfluidic system, FRET has also been developed using QDs [64, 79–81]. The occurrence of FRET-based optical change is observed by conformational changes in the intermolecular distance of 1–10 nm. Combining the advantages of using FRET-based optical changes in a molecular assay and the unique properties of QDs, a more optimum measurement system has been created [64, 79–81]. QDs are generally used as donor molecules in FRET assays [60, 82, 83]. In affinity-based interactions with sandwich assay format, the combination of direct incoming excitation fluorescence and fluorescence detected by resonance energy transfer is measured. The integration of FRET assay and microsystem is offered to overcome some of the challenges with bulk and mesoscopic methods [82]. These challenges usually consist of passivating the QDs against

non-specific adsorption, slow kinetics of hybridization (e.g., 1 h), and limited use in practice.

QD-based FRET integration with affinity biosensing is used to sense proteins, peptides, nucleic acids, and small molecules by utilizing the affinity between bioelement and analyte. Analytes or bioelements are labeled by QD-dye or QD-QD to design a FRET sensing mechanism obtaining donor and acceptor molecules by QD or dye [82]. There are affinity binding examples of creating a donor molecule by labeling the recognition element with QD to create a FRET-based biosensor mechanism; these are nucleic acid hybridization [84], affinity binding between transcription factors-double stranded DNA [85], aptamer-analyte [86], and antibody-antigen [87]. In terms of the microfluidic approach, studies on FRET-based detection by QDs are very rare. In one of the related studies, an optical system in a QD-based microfluidic system was developed capable of detecting breast cancer-specific miRNA and supporter DNA with time-resolved FRET in which a fluorophore was monitored over a period of time after a gating delay at a particular wavelength [81]. In this study, selective and sensitive results were obtained with the biosensor developed in serum tests (R^2 is 0.9408 and 0.9525, for miRNA and supporter DNA, respectively).

While biomolecules have an optical response by labeling them with QDs, in some studies, fluorescence emission is utilized after the target and QD-labeled receptor molecule hybridization by fluorescence quencher role of materials such as graphene oxide (GO). GO-QD-linked molecules, which are usually oligonucleotides or aptamers, containing ssDNA structure, produce fluorescence quenching by π - π stacking. The reason of quenching is the non-radioactive electronic excitation energy transfer between the QD and GO (FRET process), and its large absorption cross-section. When the target molecule is sent onto the quenched QD-GO-receptor complex structure, the established quenching is distorted due to the target molecule-receptor interaction and fluorescence emission occurs at the correlation of target molecule concentration. Mesoporous silica nanoparticles (MSNs) were modified with QDs and aptamers causing fluorescence quenching on GO by π - π stacking with ssDNA [63]. Later, the specific interaction of aptamers in the ssDNA structure with cells of different concentrations reduced the fluorescence quenching and caused fluorescence emission proportional to the cell concentration (see Fig. 1). Ara h1 protein, which is a peanut allergen, was detected in the microchannel with GO and QD-conjugated to the aptamer [64].

3.2 Electrochemical affinity biosensors by quantum dots in microfluidic system

QDs are most commonly used as labeling agents for bio-imaging and biosensing to take advantage of their optical features and stability; however, QDs have also interesting

electrochemical properties. To develop both catalytic [88] and affinity [14, 89, 90] based electrochemical biosensors, QDs offer some advantages in electrochemical biosensing near its optical advantages which are sturdy chemical inertness, high detection sensitivity, ECL emission properties, inherent miniaturization, and low power requirements [9].

Photoelectrochemical (PEC) sensors have attracted attention in different areas which are the clinical diagnosis, biological research, and biodefense applications. In the past few years, large optical cross-sections and tunable bandgap due to the quantum size attract prominent attention in electrochemical biosensing platforms. Graphene-QD hybrid materials are examined in photoelectrochemical changes for sensing applications. In addition to affinity-based assays, graphene-QD hybrid structures have also been studied in catalytic measurements [91]. In addition to graphene, other graphitic nanomaterials and QD-based hybrid structures are also gaining importance in bio-imaging and biosensor studies. It was reported that the composite form of 2D hexagonal Boron Nitride (h-BN) with graphene-QD can be used as a biological probe for intracellular imaging [92]. QD hybrid structures with graphitic Carbon Nitride (CN) nanomaterials change the photocatalytic effect of active sensing surface when excited in visible light [93]. Thus, the PEC signals of the biosensor are to be amplified (see Fig. 2). In order to highlight this issue, photoelectrochemical tetracycline (TET) determination was performed by immobilizing TET binding aptamer to the hybrid structure formed with graphitic- C_3N_4 (g- C_3N_4) and CdS QDs [94]. In this study, the amount of TET could be determined in the range of 1.0×10^{-8} – 2.5×10^{-7} M and the detection limit decreased to 5.3×10^{-9} M. A more sensitive biosensor was developed with the hybrid structure of g- C_3N_4 and CdS QDs compared to different methods of TET determinations. Prostate specific antigen (PSA) was detected immunologically by hybrid g- C_3N_4 @Carbon QDs with Cu nanostructures. Due to the strong coordination between Cu^{2+} ions and the hybrid structure, a decrease in photocurrent was observed in proportion to the amount of Cu bound to PSA. When the ELISA test was compared with the new biosensor with a linear measuring range of 0.02–100 ng/mL and LOD of 5.0 pg/mL, results are matched successfully [95]. In another study, by using the quenching of the PEC signals on the CdS@g- C_3N_4 hybrid structure by means of Cu^{2+} ions, a linear detection range of 1.0×10^{-11} – 5.0×10^{-8} g/mL and LOD of 4.0 pg/mL was achieved in the immunological detection of PSA [96]. The electrochemical detection method was also used for heavy metal detection, which can be reduced with a certain voltage and accumulated on the electrode. Then, reoxidation of these ions induces voltammetric signals which are interpreted as the presence of heavy metal. Based on this principle, the receptor molecules labeled with QDs containing heavy metals in their cores, which are usually DNA, aptamer or an antibody, can be determined by stripping voltammetric analysis by detecting the QDs bound on the target molecule concentration [97–100]. When QDs which

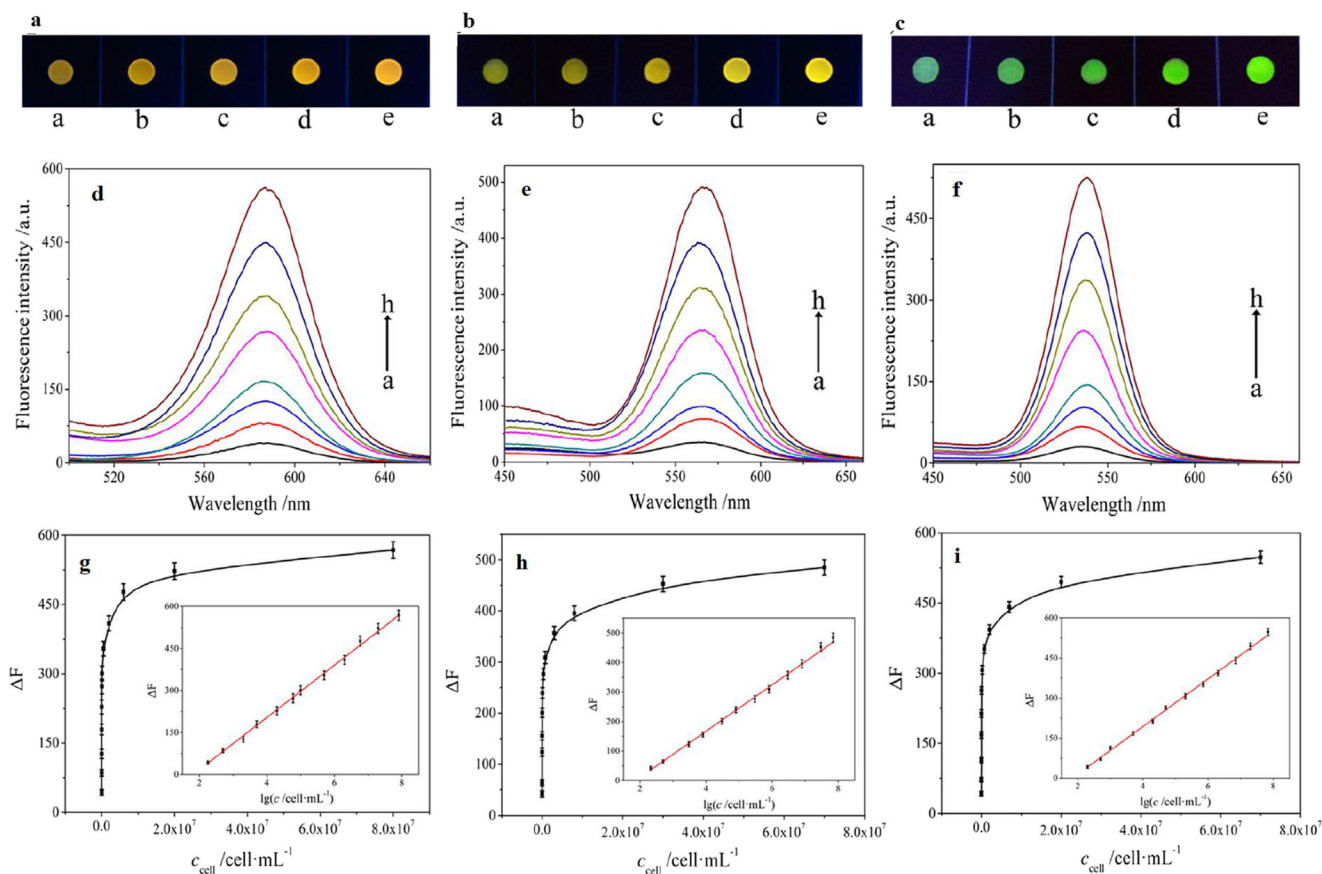


Fig. 1 Fluorescence photographs of probes incubated with different concentrations (a) MCF-7 cells (from a to e: $180, 2 \times 10^3, 2 \times 10^4, 10^5,$ and 2×10^6 cells/mL, respectively), (b) HL-60 cells (from a to e: $210, 3 \times 10^3, 3 \times 10^4, 3 \times 10^5,$ and 3×10^6 cells/mL, respectively), and (c) K562 cells (from a to e: $200, 10^3, 2 \times 10^4, 2 \times 10^5,$ and 2×10^6 cells/mL, respectively). Fluorescence emission change after quenching QD fluorescence with GO structure at the end of hybridization of aptamer and cells at different concentrations, (d) MCF-7 cells (from a to h: $0, 180, 500, 2 \times$

$10^3, 2 \times 10^4, 10^5, 2 \times 10^6,$ and 2×10^7 cells/mL, respectively), (e) HL-60 cells (from a to h: $0, 210, 500, 3 \times 10^3, 3 \times 10^4, 3 \times 10^5, 3 \times 10^6,$ and 3×10^7 cells/mL, respectively) and (f) K562 cells (from a to h: $0, 200, 500, 10^3, 2 \times 10^4, 2 \times 10^5, 2 \times 10^6,$ and 2×10^7 cells/mL, respectively). Logarithmic calibration curve for (g) MCF-7 cell, (h) HL-60 cells and (i) K562 cells. Reprinted with permission from Ref. [63]. Copyright © 2016 Elsevier

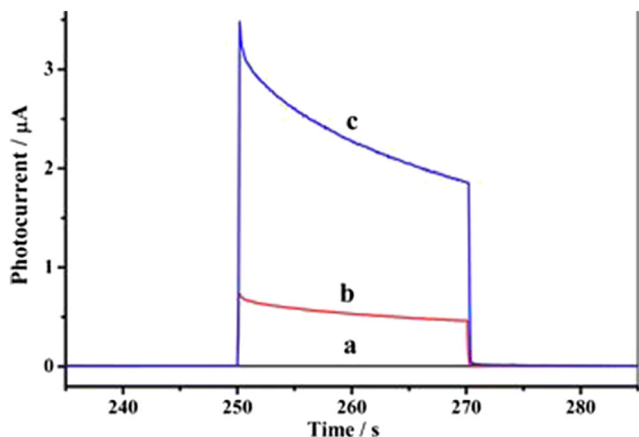


Fig. 2 PEC signals from F-doped SnO₂ conducting glass modified with hybrid structures (a) g-C₃N₄, (b) CdS, (c) g-C₃N₄@CdS. Reprinted with permission from Ref. [94]. Copyright © 2016, American Chemical Society

have different reduction potentials are tagged to different sensing molecules, simultaneous multiple detections can be achieved [101]. In electrochemical affinity-based assays developed by QD labeling which includes Cd, Zn, Pb in the core, reduction of ions like Cd²⁺ ions to Cd⁰, Zn²⁺ ions to Zn⁰ and Pb²⁺ ions to Pb⁰ from the QDs occurs an accumulation on the working electrode [102]. The further reoxidation of Cd⁰ to Cd²⁺, Zn⁰ to Zn²⁺, and Pb⁰ to Pb²⁺ give the electrochemical response to be used as a voltammetric analytical signal. It is an acidic solution to release the metal ions required for the first step. In a QD-labeled sandwich assay, when the Cd, Zn, and Pb containing QDs were dissolved, Cd²⁺, Zn²⁺, and Pb²⁺ were detected by square-wave stripping voltammetry to enable the quantification of target molecules in affinity interaction. In particular, the affinity-based biosensing is based on QD labels due to an electrochemical signal by stripping analysis, because QDs exhibit sharp and well-resolved stripping voltammetry signals with the well-defined oxidation potentials of the metal components. Ultrasensitive electrochemical affinity biosensors have been

developed as nano-tracers with a low detection limit of stripping analysis [14, 70, 90, 103, 104]. A biosensor to detect PSA protein and DNA was developed in a microfabricated tin-film electrode using Cd-ion detection by stripping voltammetry technique after labeling biomolecule with CdSe/ZnS QDs [105]. After microfabrication of electrode on Si wafer by lithography and Tin sputtering, the sensing area was functionalized with a biotinylated reporter antibody which is specific to PSA for sandwich-type immunoassay and biotinylated oligonucleotides which is used to detect C₅₃₃G mutation of the RET gene. Streptavidin-conjugated CdSe/ZnS QDs were used for labeling biotinylated biomolecules and quantification of the analytes was performed through an acidic dissolution of the QDs. The released Cd(II) was analyzed in an electrochemical cell by square-wave anodic stripping voltammetry as seen in Fig. 3. Linear detection range for PSA and DNA are 0–50 ng/mL and 0–300 nmol/L, and LODs for each are 0.12 ng/mL and 0.08 nmol/L, respectively.

An electrochemical aptasensor was also reported to detect fumonisin B1 (FB1) and OTA (Ochratoxin A) at the same time, based on magnetic beads and CdTe or PbS QDs [106]. The sensing mechanism is similar to a competitive ELISA [107]. In the presence of targets, the aptamer prefers to form the target-aptamer complex structure, thus it results in releasing of preloaded QD labels from magnetic beads. The number of QD labels remained on magnetic beads is inversely proportional to the toxin concentration in the sample. Dissolved metal ions in QDs which are Pb⁺² and Cd⁺² easily collected by an external magnetic field measured by square wave voltammetry stripping technique. LOD of this sensor was 20 pg/mL and 5 pg/mL for FB1 and OTA respectively and it was proved to be very effective for testing in the real sample (maize).

The collaboration of microfluidic technology and electrochemistry provides quasi automated measurements. The advantages of these platforms in comparison with standard procedures are reduced time of incubation steps, low volume consumption, miniaturization of whole biosensing concept, shortening response time, simplicity in usage, enabling to

measure multi targets [14], and multi analyzer on unique platform [108]. Microfluidic channels could be easily reusable by flushing and removing the particles then introducing fresh solutions or solutions of carrier supports [72, 109, 110].

4 Design and fabrication of microfluidic channels for QD-based affinity biosensors

Optical and electrochemical affinity-based detection studies in the microfluidic system are reviewed in Table 1 and these designs were examined in details. Design and fabrication details for affinity-based microfluidic technology as given in Sections 3.1 and 3.2 will be examined in this section. Microfluidic platforms are combination of micro-channels by design for specific applications. In the fabrication of microchannels, the common material polydimethylsiloxane (PDMS) which is a silicon-based organic polymer is used owing to its good elastic properties, non-toxicity, biocompatibility, optical transparency, non-flammability, chemical inertness, as well as conformability. In these studies, an active sensing region was created in the microfluidic system where the optical changes resulting from the interaction of the target molecule and QD-conjugated bioelement occurred or interactions were observed in the channel with the flow [55]. Optical and electrochemical biosensors have been developed by modifying the channel surface (deposition of conductive surface, or chemical modifications) in microsystems or by developing the sensor region with functionalized carrier solid supports (magnetic particles, polystyrene microspheres) with an appropriate design in the microchannel (microwells, microchambers) where a stable active detection zone is created [15, 54]. A microfluidic system design that performs optical detection as a result of fluorescent emission after Ab–Ag–QD interaction on the carrier solid supports is shown in Fig. 4a. In the microfluidic system developed without the use of a carrier solid support, the detection zone is activated in a specific area of channel surface by immobilization techniques. Different channels and sensing regions on the same chip

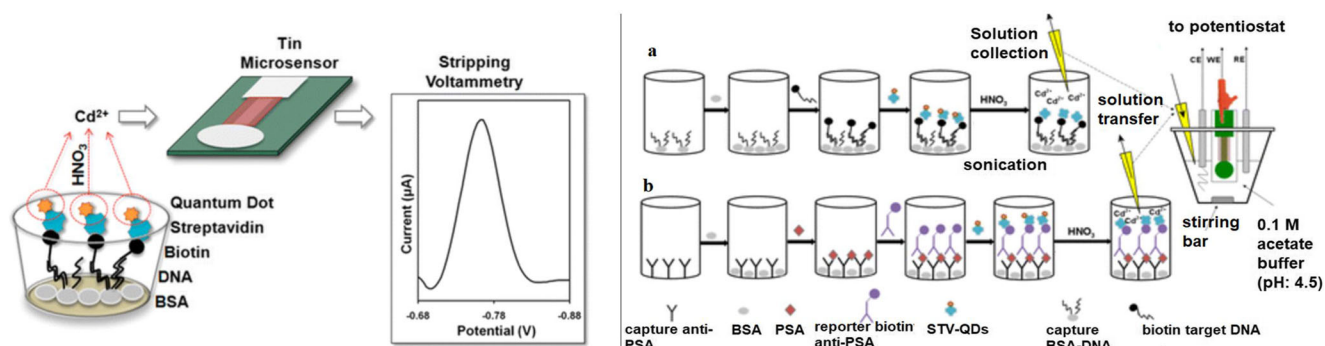


Fig. 3 Schematic presentation of the electrochemical immunoassay procedure. (a) Electrochemical affinity assay for the detection of C₅₃₃G mutation of RET gene and (b) electrochemical immunoassay for the

detection of PSA in human serum. Reprinted with permission from Ref. [105]. Copyright © 2013, American Chemical Society

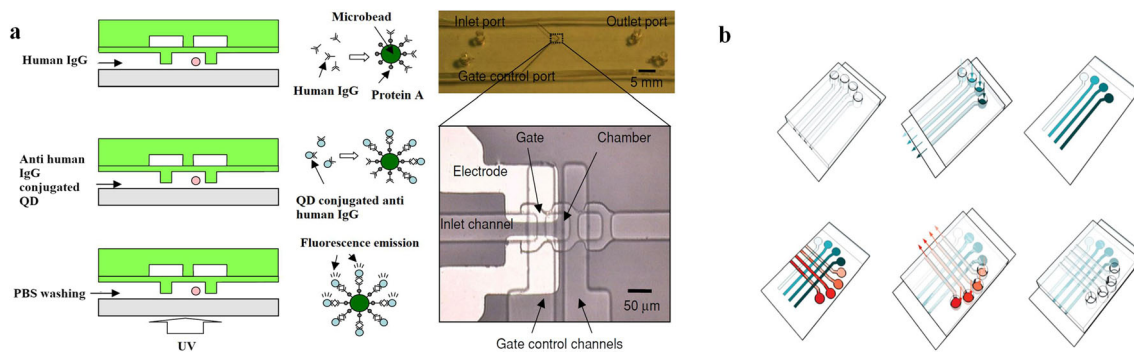


Fig. 4 (a) hIgG injection from the inlet of the microchannel, anti-hIgG conjugated QD injection and washing step (left), microscopy image of microchannels (right) Ref. [54]. (b) Protein chip designed by

immobilizing antibody to the surface of the PDMS channels. Reprinted with permission from Ref. [57]. Copyright © 2010, American Chemical Society

was developed (see Fig. 4b) to detect more than one antigen in the microfluidic system [57].

Fluorescent microscope [54, 57], fiber optic system [15, 60, 111], and spectroscopic system integration [55] were also used to analyze the fluorescence intensity. Figure 5 shows the integration of the fiber optic detection system into the microfluidic system tracer to detect the Ab–Ag–QD interactions in the microfluidic system [111]. LED light sources are integrated onto the system to excite the QDs at a certain wavelength and fiber optic cables are used to collect the emitted light beam [62]. Photomicrographs are used to analyze optical signals from microarray designs [56]. In the design of microsystems for the detection of target molecules with a fluorescence-labeled biomolecule, the fluorescence change resulting from biosensing has recently been made easy to analyze by integrating it with a smartphone video processing [112].

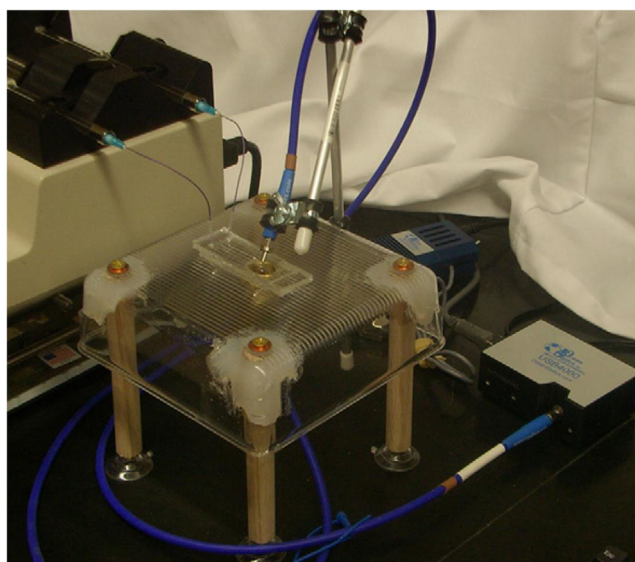
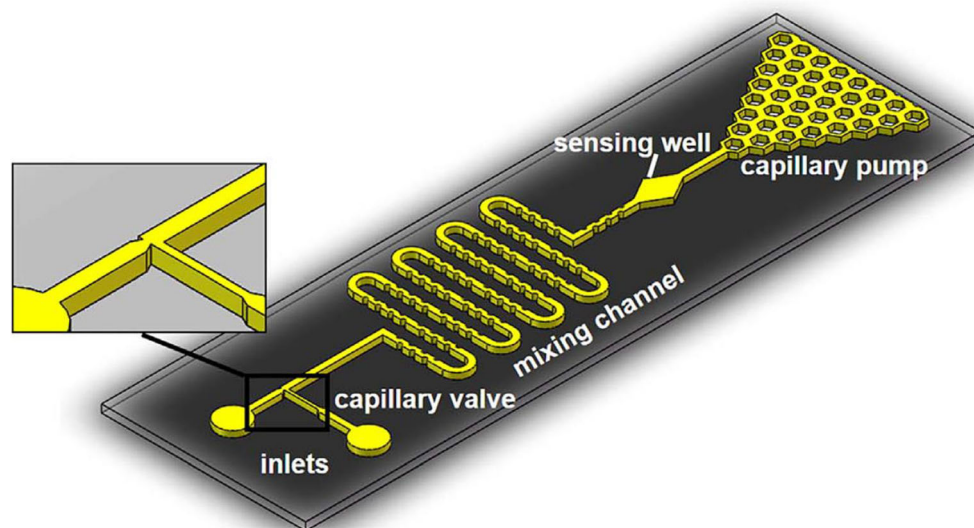


Fig. 5 Fiber optic system integrated to microfluidic system, light source, and syringe pump from Ref. [111]

4.1 Development of biosensor by QD in microchannels or on modified substrates

The signal transduction system of electrochemical biosensors developed using QDs in the microfluidic system is the similar approach as being used in traditional electrochemical measurement methods. Commonly used electrochemical transduction methods are electrochemiluminescence analyzer [89], square wave voltammetry [14, 70], cyclic voltammetry [70, 89, 108], electrochemical impedance spectroscopy [73, 89], differential-pulse voltammetry [108], and chronoamperometry [108]. Optical and electrochemical studies performed directly on the microchannel surface or inside the microchannel, without using any carrier support, will be explained with examples in this section. In the design of the microfluidic biochip shown in Fig. 6, the microfluidic chip was consisted of two inlets, a mixing/incubation channel, sensing well, and a capillary pump [64]. Capillary pumping is an attractive means of liquid actuation because it is a passive mechanism. Flow rate in capillary action generally depends on viscosity of the liquid sample and its surface energy. The self-sampling can be generated by these hexagon-shaped capillary pumping by means of splitting the capillary action into hundreds of smaller parallel microchannels. Design of the capillary-driven retarding valve at the entrance of the mixing/incubation channel avoids air capture in the microchannel when dispensing the QD–aptamer–GO probe mixture and the Ara h1 sample into the inlets. A zigzag microchannel was designed to mix the samples in the microchannel efficiently. The sensing well was designed as a diamond-shaped well which was aligned to the sensing window of the Si photodiode. PDMS channels were produced by standard lithography technique and then kept in bovine serum albumin (BSA) solution to prevent the non-specific adsorption of the desired proteins onto the microchannel walls. Later, oxygen plasma was combined with the glass substrate to cover the microfluidic system. In this design, reference fluorescence density was recorded in the detection zone by introducing QD–aptamer probes with a GO solution and Ara h1 protein at standard concentration. Then, when the concentration of the

Fig. 6 Design of a QD–GO quenching biosensing system in microfluidic system. Reprinted with permission from Ref. [64]. Copyright © 2016 Elsevier



targeted protein changed, the fluorescence intensity was measured with response characteristics.

An electrochemical biosensor was developed in a microfluidic system that can analyze two different biomarkers simultaneously by detecting Cd^{2+} and Zn^{2+} ions with square-wave anodic stripping voltammetry [14]. An immunoassay in the microreactor is formed by PDMS–GNP composite structure with two different antibodies labelled QDs and its response is seen in Fig. 7. PDMS–gold nanoparticles are composed on the basis of the reductive property of PDMS. PDMS–GNP is shaped in a series of holes on another composite film to produce the microreactors integrated with Ag/AgCl reference electrode, a Pt wire counter electrode, and a carbon fiber working electrode. Affinity reaction occurs between antibodies for cTnI and CRP, antigens (cTnI and CRP), and QD-conjugated secondary

antibodies (CdTe QD–anti-cTnI, ZnSe QD–anti-CRP). After the injection of acidic solution through microreactors, ions from QDs are released and their transduction is measured by square-wave anodic stripping voltammetry.

In an electrochemical analysis in the microfluidic system, electrodes are integrated with microchannels. Electrodes with a thickness of 4–5 μm are fabricated on the microchannel surface with screen printing technology and modified with various immobilization techniques allowing electrochemical biosensing within the microchannel [70]. In the microfluidic system, electrochemical deposition methods, chemical modifications, and entrapment of biomolecules on the electrode with the help of nanoporous membranes [73] also create very versatile active sensing zone on the electrode surface.

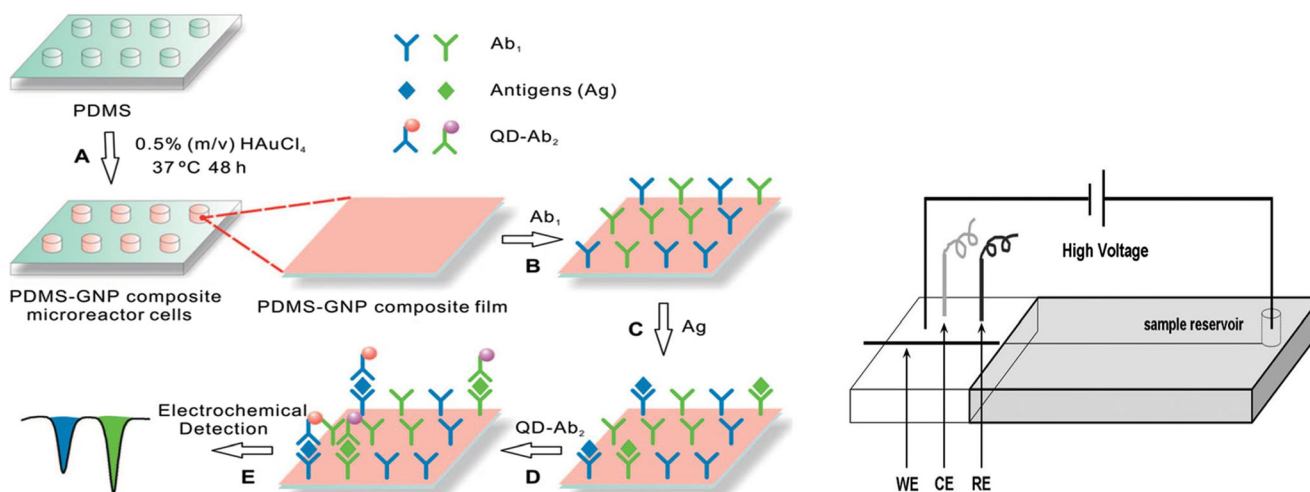


Fig. 7 (left) Schematic diagram of in situ synthesis of PDMS–GNP composite microreactors and immunoassay analytical procedure based on QD label. (right) Schematic representation of the electrochemical analysis via the flow injection mode on the microchip Ref. [14]

4.2 QD-modified carrier solid support-based microfluidic designs

Optical biosensors have been fabricated by developing the sensing region with functionalized carrier solid supports (magnetic particles or polystyrene microspheres) with an appropriate design in the microchannel (microwells, microchambers) where a stable active detection zone is created [15, 54]. A microfluidic system design that performs optical detection as a result of fluorescent emission after Ab–Ag–QD interaction on the carrier solid supports is shown in Fig. 4a. In this study, hIgG-immobilized microspheres were placed in microchambers and entrapped with help of the pneumatic valves (negative pneumatic pressure/vacuum). Entrapment and next step modification can be obtained in the designed microchambers. The QD-conjugated anti-hIgG in solution-driven from inlet channel interacted with the microspheres in the micro chamber then the UV-induced QDs emitted fluorescent light was measured [54].

4.2.1 Magnetic carrier particle-based designs

On-chip magnetic bead manipulation designs are also utilized for the development of QD-based electrochemical and optical biosensors [70]. Magnetic beads into microfluidic platforms to sense viruses, biomolecules, cells, and environmental pollutants have been widely reported in the literature [113–116]. Biomolecules to detect analytes have been labeled mainly with enzymatic and fluorescent labels for their posterior detection by magnetic beads. In systems using magnetic carrier solid supports, Ab–Ag–QD interaction was observed on the magnetic particle where they are held in a certain area of the channel with the help of a magnet [15]. The detection zone in microfluidic system is a section of localized magnetic carriers by means of externally applied magnetic field. As a result of the interaction in this region, the change in QD fluorescence is detected as shown in Fig. 8 [62]. Targeted structure of bacteria and magnetic particles at the detection zone was localized at the end of long separation chamber with dimensions of length of 11 mm, width of 3 mm, and height of 1 mm after passing through mixing and incubation channels [67]. QDs were released from the complex structure by introducing GSH into the system from the 3rd entrance and then the fluorescence intensity of the QDs was analyzed. Serpentine-shaped microchannel designs aim to mix materials and enable proper incubation and interaction efficiently [62]. In some studies, it was performed by making various patterns like convergence–divergence within the serpentine channel to make micro-mixing even more efficient as seen Fig. 9 [67].

4.2.2 Polymeric beads as a carrier in microfluidic QD-based biosensor

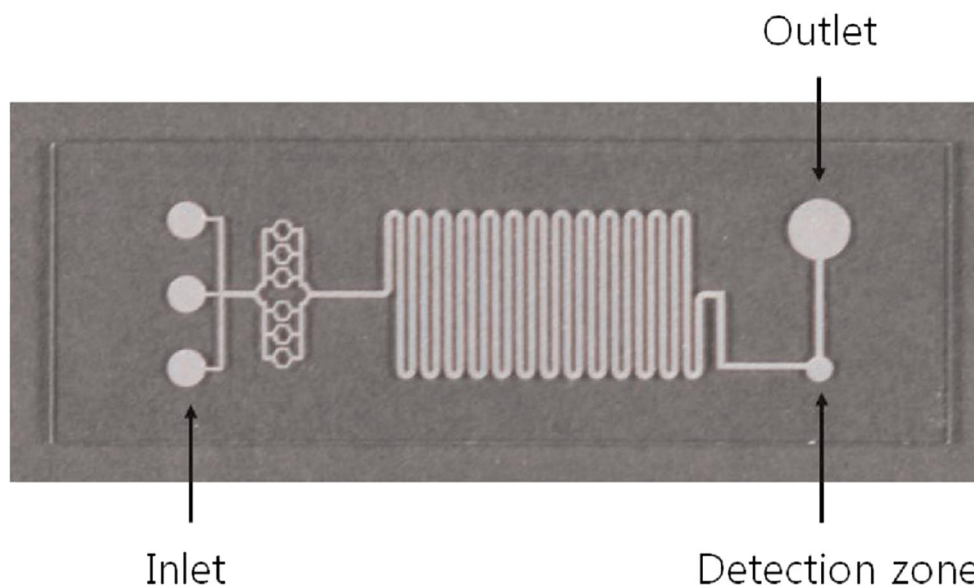
A microfluidic system design that performs optical detection as a result of fluorescent emission after Ab–Ag–QD interaction on the polystyrene carrier solid supports is shown in Fig. 4a. Microchamber of 50 μm \times 50 μm square by area and 30 μm by height was designed to entrap a functionalized polystyrene microbead (10 μm diameter). The pneumatic gates are manufactured to create a 5 μm opening to the bottom of the channel, so that the liquid flows through the microbead chamber while it cannot go outside [54]. Polystyrene bead-based biosensor was designed for DNA detection by QDs by two PDMS slabs [58]. The design consisted of ten trapping chambers with an independent channel to confine functionalized microbeads and to inject sample by a simple microfluidic channel. These ten different trapping chambers are the individually addressable reservoir for functionalized microbeads with different probes to obtain a platform of simultaneous multiple detections as shown Fig. 10. Biotinylated target RNAs immobilized on beads are sent to chambers and then streptavidin-bound QDs flow through the beads in order to observe any possible fluorescence change. With this design, different genotypes with few base differences could be distinguished.

4.2.3 Bead-based microarray systems in microfluidic system

In order to develop a microarray system, microwells are formed by etching on the microchannel substrate and modified polystyrene beads are placed inside, and then fluorescence density is observed with the help of QDs. In case of bead-based microarray system design, detection of multi-antigen is enabled with QDs that emit different wavelengths by modified different antigens [56, 61].

NBC (Nano-bio-chip) was developed in a microarray design which was integrated with QDs and the system was compatible with complex fluids (serum, saliva) [56]. The Si substrate ((100) surface oriented wafers) of the microfluidic channel has been anisotropically etched to place agarose beads, which were used as solid-phase support. NBC simultaneously detected different cancer biomarkers, and served as a sensitive and specific cancer diagnostic tool for use with both serum and saliva samples. In Fig 11, NBC design is explained in details, each bead is individually located into well on the silicon surface, and bead specificity was determined by the type of antibody covalently bound to bead (see Fig. 11a). NBC chip was consisted of precision-cut layers designed for reagent delivery (Fig. 11b). Reagents were delivered through the top inlet of the flow cell apparatus, and passed through the agarose beads and then nonreactive reagents were accumulated in waste that was the lower port. The intensity of the fluorescence signal

Fig. 8 A microfluidic chip design with magnetic carrier supports which are collected in the detection zone by help of external magnetic force. Reprinted with permission from Ref. [62]. Copyright © 2014 Elsevier



correlated directly to the amount of antigen present in the sample as shown in Fig. 11d. Nine bead replicates were captured with a concentration of 1.0 mg/mL antibody, and three beads were selected as control ones with isotype antibody. Noise was determined by three isotype control beads, the mean of the nine beads was defined as a signal, and background signal was determined as output from biomarker-specific beads in the absence of antigen. In NBC sensing platform, response time is 27 min, linear detection ranges are 0–100 ng/mL, 0–60 ng/mL, and 0–400 U/mL for CEA, Her-2/Neu, and CA125, respectively.

4.2.4 QD integrated micro-paper-based analytical device (μ PAD)

As an alternative to PDMS, glass, and PMMA materials, which are frequently used in microchannel fabrication, paper microchannels are also preferred due to their advantages

[117–119]. The most important advantages of these paper-based microsystems, which are called μ PAD (paper-based analytical device) systems, are the convenience of miniaturization, automation, and integration, low cost, facile portability, quick detection in the field, easy to fabricate according to other microsystem materials and disposability. And there is no need for an external drive pump to operate μ PADs, and fluid flow is driven just by the paper's capillary force with the aid of hydrophilic channels. Various transduction techniques in biosensors (electrochemical, optical, surface enhanced Raman spectroscopy [120], and colorimetry [121]) are integrated with PAD systems. In the patterning of microchannels, hydrophobic/hydrophilic surfaces or functionalized surfaces are frequently fabricated by means of the wax patterning [122, 123] and screen printing techniques [108]. On the patterned surfaces, optical and electrochemical biosensors have been developed with the modifications made with QDs. A design of μ -PAD was fabricated to detect three different cells

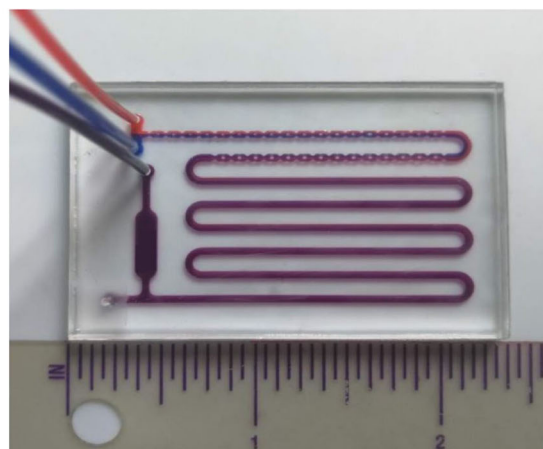
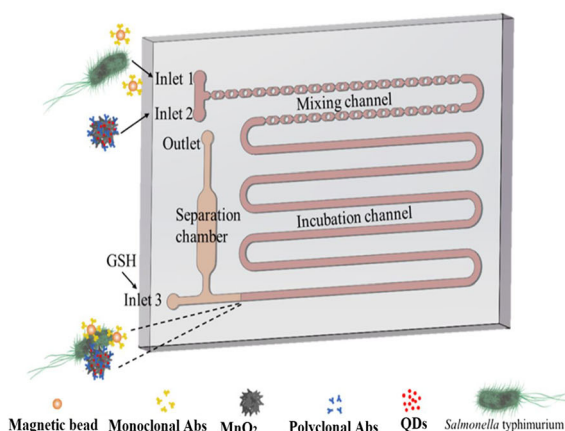


Fig. 9 A design that allows Salmonella bacteria to be bound with magnetic particles and combined with MnO₂-QD complex structure to detect GSH and QD in the separation chamber of the microfluidic system. Ref. [67]

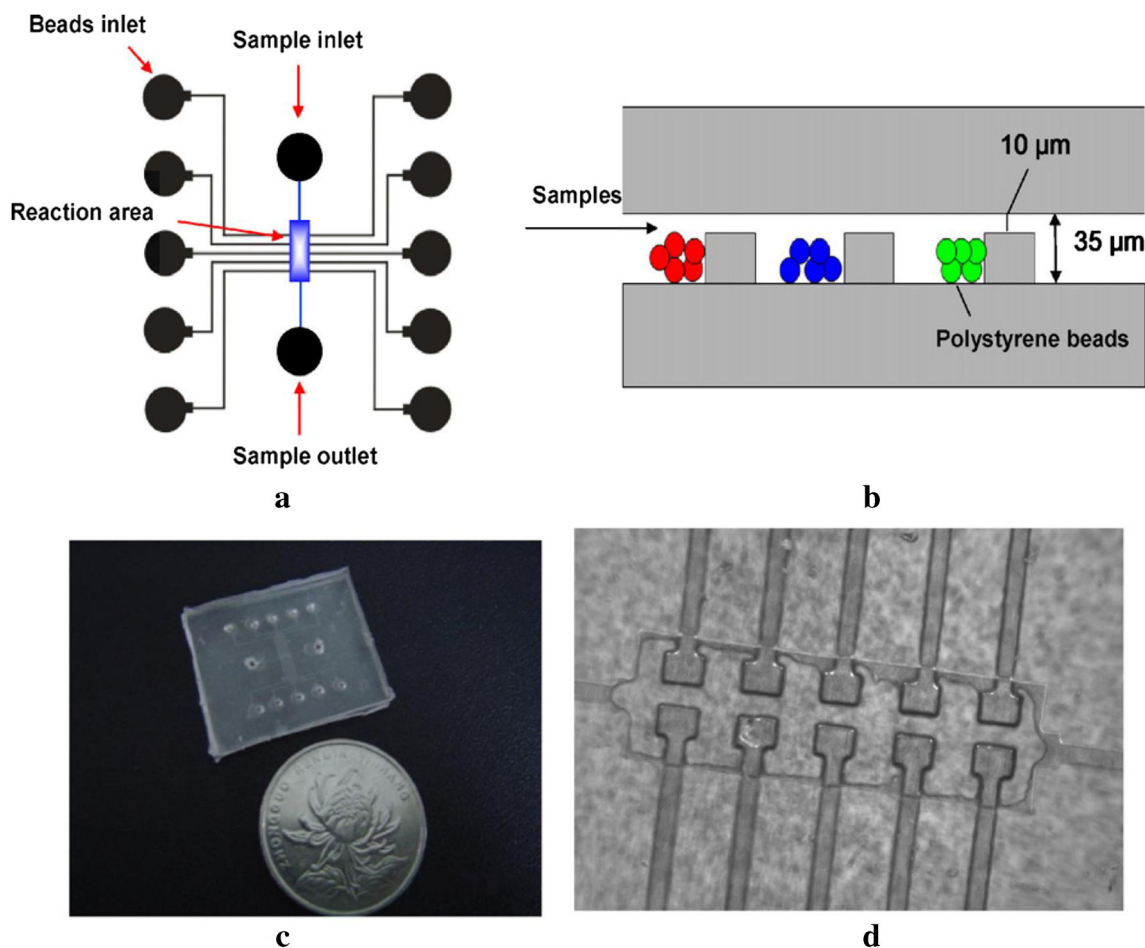


Fig. 10 Microfluidic chip with microbead array for virus DNA analysis. (a) An overview of the microfluidic chip design. (b) A cross section of the reaction and detection area. (c) Photograph of the microchip. (d) A

microscope image of the reaction area. Reprinted with permission from Ref. [58]. Copyright © 2010 Elsevier

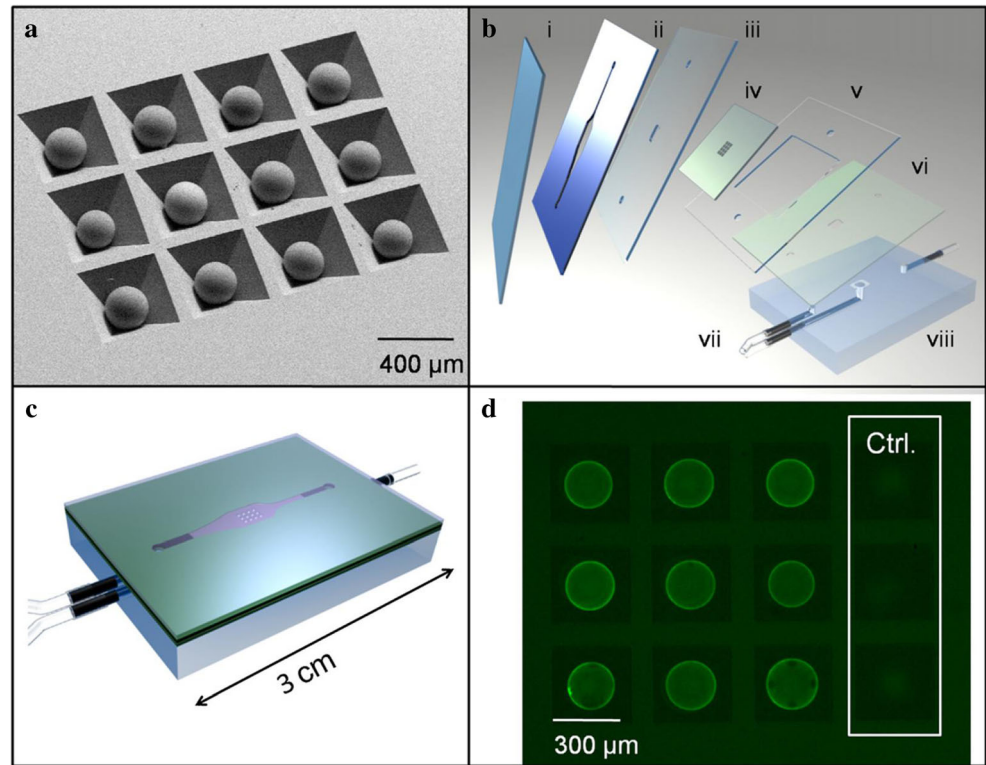
[63]. By modifying MSNs with QDs and aptamers specific for different cells (MCF-7, HL-60, and K562), qualitative and quantitative biosensors have been developed in order to measure different color emissions in separate chambers as shown in Fig. 12. In this study, an effective fluorescence quencher role of GO was utilized by modifying the paper-based surface with GO in order to obtain a visible qualitative response of optical signals. MSNs modified by QDs and aptamers resulted in fluorescence quenching on GO by π - π stacking with ssDNA. Then, the specific interaction of the ssDNA structure in aptamers with the cells prevents fluorescence quenching and induces fluorescence emission.

In another study, an optical biosensor was developed using ZnSe QDs to detect Cd^{2+} and Pb^{2+} ions by combining the PAD system with ion imprinting technology [68]. Ion imprinting was obtained with APTES and tetraethoxysilane (TEOS) monomers on the glass fiber paper using Cd^{2+} or Pb^{2+} ions as templates. After polymerization and elution of the template ions by an acidic solution, crosslinking around Cd^{2+} or Pb^{2+} ions provide the cavity to recognize Cd^{2+} or Pb^{2+} ions.

5 Future perspective

Infectious diseases have been very fatal and detrimental to people and their civilizations throughout the history. They caused high global health and economic challenges in the last two decades. COVID-19 pandemic has presently affected all aspects of daily life comfort together with stressed economy and health problems in the world. Thus, it is extremely critical to deal with any type of future pathogenic breakthrough in a reliable and manageable manner. The best way to struggle against the spread of an infectious disease is to develop adaptable, cheap, easy-to-use, portable, accurate, and reliable technological platforms, so that early detection of infectious diseases will be achieved in a timely and effective manner. The prompt adaptability of miniaturized fluidic detection systems to QD-based biosensor applications may increase hope for the accelerated development of new detectors for COVID-19 and different future threads. This is quite possible, because recent molecular studies on the COVID-

Fig. 11 (a) SEM images of beads in anisotropically etched silicon chip. (b) Chip (iv) is fitted between double-sided adhesive layer (ii) and cover slip (i) with laminate layers (iii, v, vi) included to direct fluid flow through PMMA base (viii) and inlet and outlet ports (vii). (c) Sealed LoC assembly. (d) Fluorescent image of beads after immunoassay including negative controls as imaged with one second of CCD camera integration (exposure) time. Reprinted with permission from Ref. [56]. Copyright © 2009 Elsevier



19 virus have already revealed viral genetic material, viral proteins, and antibodies of the coronavirus. Unfortunately, there are few studies of using QDs to diagnose viruses, including COVID-19, in a microfluidics system through conjugation of QDs with corresponding biomolecules. However, it is a very promising, since QD-based biosensor-adapted systems would be designed in a molecular level in order to capture targeted virus in an efficient way. Thus, the research and then commercialization are expected to be materialized in a very short term.

Moreover, affinity-based biosensors could be designed in a way that multi-virus detection would be possible due to flexibility of QD design and fabrication of microfluidics. The other important features of possible biosensors for COVID-19 are adaptability to CMOS devices and integration to flexible substrates. Finally, researchers should also consider the adaptability of COVID-19 diagnostic biosensors to smartphones, therefore biosensor-based diagnostic would be commonly utilized in a daily life.

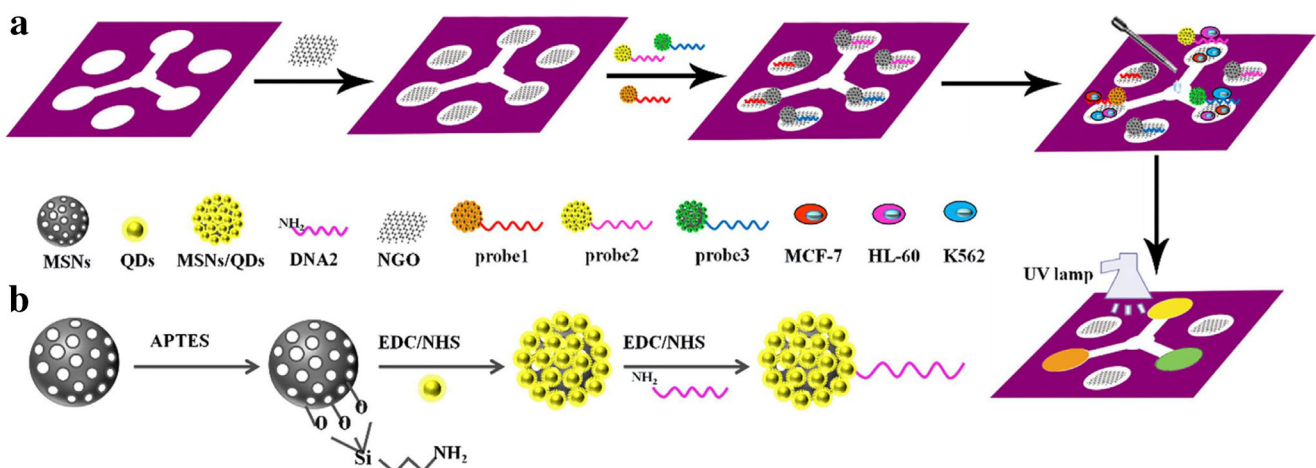


Fig. 12 Schematic representation of QD based μ -PAD design and fabrication allowing multiple detection. Reprinted with permission from Ref. [63]. Copyright © 2016 Elsevier

6 Conclusion

QD fluorophores promise to help overcome some of the challenges in biosensor applications with their high quantum yields. QD integration in biosensor applications is highly being encouraged and the most appropriate platforms are being developed for the improvement of QD stability and lifetime in biosensor applications. Microfluidic systems take an important place as a platform in QD integration for biosensing applications. A QD-based biosensor integrated with the microfluidic system can be used in point of care through its instrumentality and portability. These portable designs can provide reliable and fast detection in environmental issues and the biomedical field. As a critical development in this field, if the desired detection platform is integrated with QDs and microfluidic systems, more efficient results can be obtained in fast and portable detection systems. When we consider the COVID-19 pandemic that we have been struggling with recently, it has a great importance to make rapid and widespread detection with high versatility and accuracy. In such an integration, combined effect of use of microfluidics system and QDs will help us better understand the importance of their contributions to deal with pandemic conditions in terms of PoC techniques.

References

- S. Zhu, J. Zhang, C. Qiao, S. Tang, Y. Li, W. Yuan, B. Li, L. Tian, F. Liu, R. Hu, H. Gao, H. Wei, H. Zhang, H. Sun, B. Yang, Strongly green-photoluminescent graphene quantum dots for bioimaging applications. *Chem. Commun.* **47**(24), 6858–6860 (2011). <https://doi.org/10.1039/C1CC11122A>
- J. Ruan, H. Song, Q. Qian, C. Li, K. Wang, C. Bao, D. Cui, HER2 Monoclonal antibody conjugated RNase-A-associated CdTe quantum dots for targeted imaging and therapy of gastric cancer. *Biomaterials* **33**(29), 7093–7102 (2012). <https://doi.org/10.1016/j.biomaterials.2012.06.053>
- M.F. Frasco, N. Chaniotakis, Semiconductor quantum dots in chemical sensors and biosensors. *Sensors* **9**(9), 7266–7286 (2009). <https://doi.org/10.3390/s90907266>
- C. Yang, L. Hu, H.-Y. Zhu, Y. Ling, J.-H. Tao, C.-X. Xu, RGO Quantum dots/ZnO hybrid nanofibers fabricated using electrospun polymer templates and applications in drug screening involving an intracellular H₂O₂ sensor. *J. Mater. Chem. B* **3**(13), 2651–2659 (2015). <https://doi.org/10.1039/C4TB02134G>
- L. Zhang, Y. Sun, Y.-Y. Liang, J.-P. He, W.-W. Zhao, J.-J. Xu, H.-Y. Chen, Ag Nanoclusters could efficiently quench the photoresponse of CdS quantum dots for novel energy transfer-based photoelectrochemical bioanalysis. *Biosens. Bioelectron.* **85**, 930–934 (2016). <https://doi.org/10.1016/j.bios.2016.06.018>
- S. Su, J. Fan, B. Xue, L. Yuwen, X. Liu, D. Pan, C. Fan, L. Wang, DNA-conjugated quantum dot nanoprobe for high-sensitivity fluorescent detection of DNA and micro-RNA. *ACS Appl. Mater. Interfaces* **6**(2), 1152–1157 (2014). <https://doi.org/10.1021/am404811j>
- E. Sartorel, C. Ünü, M. Jose, A. Massoni-Laporte, J. Meca, J.-B. Sibarita, D. McCusker, Phosphatidylserine and GTPase activation control Cdc42 nanoclustering to counter dissipative diffusion. *Mol. Biol. Cell* **29**(11), 1299–1310 (2018). <https://doi.org/10.1091/mbc.E18-01-0051>
- K.F. Fox, C. Ünü, V. Balevičius, B.N. Ramdour, C. Kern, X. Pan, M. Li, H. van Amerongen, C.D.P. Duffy, A possible molecular basis for photoprotection in the minor antenna proteins of plants. *Biochim. Biophys. Acta BBA - Bioenerg.* **1859**(7), 471–481 (2018). <https://doi.org/10.1016/j.bbabo.2018.03.015>
- P. Devi, S. Saini, K.-H. Kim, The advanced role of carbon quantum dots in nanomedical applications. *Biosens. Bioelectron.* **141**, 111158 (2019). <https://doi.org/10.1016/j.bios.2019.02.059>
- M. Amelia, C. Lincheneau, S. Silvi, A. Credi, Electrochemical properties of CdSe and CdTe quantum dots. *Chem. Soc. Rev.* **41**(17), 5728–5743 (2012). <https://doi.org/10.1039/C2CS35117J>
- I.L. Medintz, H.T. Uyeda, E.R. Goldman, H. Mattoussi, Quantum dot bioconjugates for imaging, labelling and sensing. *Nat. Mater.* **4**(6), 435–446 (2005). <https://doi.org/10.1038/nmat1390>
- A. Valizadeh, H. Mikaeili, M. Samiei, S.M. Farkhani, N. Zarghami, M. Kouhi, A. Akbarzadeh, S. Davaran, Quantum dots: synthesis, bioapplications, and toxicity. *Nanoscale Res. Lett.* **7**(1), 480 (2012). <https://doi.org/10.1186/1556-276X-7-480>
- A.M. Wagner, J.M. Knipe, G. Orive, N.A. Peppas, Quantum dots in biomedical applications. *Acta Biomater.* **94**, 44–63 (2019). <https://doi.org/10.1016/j.actbio.2019.05.022>
- F. Zhou, M. Lu, W. Wang, Z.-P. Bian, J.-R. Zhang, J.-J. Zhu, Electrochemical immunosensor for simultaneous detection of dual cardiac markers based on a poly(dimethylsiloxane)-gold nanoparticles composite microfluidic chip: a proof of principle. *Clin. Chem.* **56**(11), 1701–1707 (2010). <https://doi.org/10.1373/clinchem.2010.147256>
- H.Y. Tsai, H.H. Wu, B.C. Chou, C.S. Li, B.Z. Gau, Z.Y. Lin, C.B. Fuh, A magneto-microfluidic platform for fluorescence immunosensing using quantum dot nanoparticles. *Nanotechnology* **30**(50), 505101 (2019). <https://doi.org/10.1088/1361-6528/ab423d>
- J. Tian, L. Zhou, Y. Zhao, Y. Wang, Y. Peng, S. Zhao, Multiplexed detection of tumor markers with multicolor quantum dots based on fluorescence polarization immunoassay. *Talanta* **92**, 72–77 (2012). <https://doi.org/10.1016/j.talanta.2012.01.051>
- T. Hu, J. Xu, Y. Ye, Y. Han, X. Li, Z. Wang, D. Sun, Y. Zhou, Z. Ni, Visual detection of mixed organophosphorous pesticide using QD-AChE aerogel based microfluidic arrays sensor. *Biosens. Bioelectron.* **136**, 112–117 (2019). <https://doi.org/10.1016/j.bios.2019.04.036>
- J. Hassanzadeh, A. Khataee, Ultrasensitive chemiluminescent biosensor for the detection of cholesterol based on synergistic peroxidase-like activity of MoS₂ and graphene quantum dots. *Talanta* **178**, 992–1000 (2018). <https://doi.org/10.1016/j.talanta.2017.08.107>
- T. Hu, L. Zhang, W. Wen, X. Zhang, S. Wang, Enzyme catalytic amplification of MiRNA-155 detection with graphene quantum dot-based electrochemical biosensor. *Biosens. Bioelectron.* **77**, 451–456 (2016). <https://doi.org/10.1016/j.bios.2015.09.068>
- P.M. Valencia, O.C. Farokhzad, R. Karnik, R. Langer, Microfluidic technologies for accelerating the clinical translation of nanoparticles. *Nat. Nanotechnol.* **7**(10), 623–629 (2012). <https://doi.org/10.1038/nnano.2012.168>
- P.U. Alves, R. Vinhas, A.R. Fernandes, S.Z. Birol, L. Trabzon, I. Bernacka-Wojcik, R. Igreja, P. Lopes, P.V. Baptista, H. Águas, E. Fortunato, R. Martins, Multifunctional microfluidic chip for optical nanoprobe based rna detection – application to chronic myeloid leukemia. *Sci. Rep.* **8**(1), 381 (2018). <https://doi.org/10.1038/s41598-017-18725-9>
- S. Colin, *Microfluidics* (Wiley, 2013)

23. U. Sonmez, S. Jaber, L. Trabzon, Super-enhanced particle focusing in a novel microchannel geometry using inertial microfluidics. *J. Micromech. Microeng.* **27**(6), 065003 (2017). <https://doi.org/10.1088/1361-6439/aa6b18>
24. S.K. Sia, L.J. Kricka, Microfluidics and point-of-care testing. *Lab Chip* **8**(12), 1982–1983 (2008). <https://doi.org/10.1039/B817915H>
25. M. Zuvin, N. Mansur, S.Z. Birol, L. Trabzon, A. Sayı Yazgan, Human breast cancer cell enrichment by dean flow driven microfluidic channels. *Microsyst. Technol.* **22**(3), 645–652 (2016). <https://doi.org/10.1007/s00542-015-2425-7>
26. T.G. Henares, F. Mizutani, H. Hisamoto, Current development in microfluidic immunosensing chip. *Anal. Chim. Acta* **611**(1), 17–30 (2008). <https://doi.org/10.1016/j.aca.2008.01.064>
27. C.H. Vannoy, A.J. Tavares, M.O. Noor, U. Uddayasankar, U.J. Krull, Biosensing with quantum dots: a microfluidic approach. *Sensors* **11**(10), 9732–9763 (2011). <https://doi.org/10.3390/s111009732>
28. B. Liu, J. Li, X. Tang, Z. Wu, J. Lu, C. Liang, S. Hou, L. Zhang, T. Li, W. Zhao, Y. Fu, Y. Ke, C. Li, Development of a quantum-dot lateral flow immunoassay strip based portable fluorescence smartphone system for ultrasensitive detection of IgM/IgG to SARS-CoV-2. medRxiv, 2020.07.21.20159392 (2020). <https://doi.org/10.1101/2020.07.21.20159392>
29. C. Wang, X. Yang, B. Gu, H. Liu, Z. Zhou, L. Shi, X. Cheng, S. Wang, Sensitive and simultaneous detection of SARS-CoV-2-specific IgM/IgG using lateral flow immunoassay based on dual-mode quantum dot nanobeads. *Anal. Chem.* **92**(23), 15542–15549 (2020). <https://doi.org/10.1021/acs.analchem.0c03484>
30. D. Leech, Affinity biosensors. *Chem. Soc. Rev.* **23**(3), 205–213 (1994). <https://doi.org/10.1039/CS9942300205>
31. A. Turner, I. Karube, G.S. Wilson, *Biosensors: fundamentals and applications* (Oxford University Press, 1987)
32. M.A. Arugula, A. Simonian, Novel trends in affinity biosensors: current challenges and perspectives. *Meas. Sci. Technol.* **25**(3), 032001 (2014). <https://doi.org/10.1088/0957-0233/25/3/032001>
33. P.B. Lippa, L.J. Sokoll, D.W. Chan, Immunosensors—principles and applications to clinical chemistry. *Clin. Chim. Acta* **314**(1), 1–26 (2001). [https://doi.org/10.1016/S0009-8981\(01\)00629-5](https://doi.org/10.1016/S0009-8981(01)00629-5)
34. J. Wu, Z. Fu, F. Yan, H. Ju, Biomedical and clinical applications of immunoassays and immunosensors for tumor markers. *TrAC Trends Anal. Chem.* **26**(7), 679–688 (2007). <https://doi.org/10.1016/j.trac.2007.05.007>
35. M. Egholm, O. Buchardt, P.E. Nielsen, R.H. Berg, Peptide nucleic acids (PNA). Oligonucleotide analogs with an achiral peptide backbone. *J. Am. Chem. Soc.* **114**(5), 1895–1897 (1992). <https://doi.org/10.1021/ja00031a062>
36. C. Briones, M. Moreno, Applications of peptide nucleic acids (PNAs) and locked nucleic acids (LNAs) in biosensor development. *Anal. Bioanal. Chem.* **402**(10), 3071–3089 (2012). <https://doi.org/10.1007/s00216-012-5742-z>
37. A. Saadati, S. Hassanpour, M. de la Guardia, J. Mosafer, M. Hashemzaei, A. Mokhtarzadeh, B. Baradaran, Recent advances on application of peptide nucleic acids as a bioreceptor in biosensors development. *TrAC Trends Anal. Chem.* **114**, 56–68 (2019). <https://doi.org/10.1016/j.trac.2019.02.030>
38. S. Song, L. Wang, J. Li, C. Fan, J. Zhao, Aptamer-based biosensors. *TrAC Trends Anal. Chem.* **27**(2), 108–117 (2008). <https://doi.org/10.1016/j.trac.2007.12.004>
39. K. Haupt, K. Mosbach, Molecularly imprinted polymers and their use in biomimetic sensors. *Chem. Rev.* **100**(7), 2495–2504 (2000). <https://doi.org/10.1021/cr990099w>
40. A. Adumitrăchioaie, M. Tertis, A. Cernat, R. Sandulescu, C. Cristea, Electrochemical methods based on molecularly imprinted polymers for drug detection. A review. *Int. J. Electrochem. Sci.* **13**, 2556–2576 (2018). <https://doi.org/10.20964/2018.03.75>
41. M. Bruchez Jr., M. Moronne, P. Gin, S. Weiss, A.P. Alivisatos, Semiconductor nanocrystals as fluorescent biological labels. *Science* **281**(5385), 2013–2016 (1998). <https://doi.org/10.1126/science.281.5385.2013>
42. W.J. Parak, D. Gerion, T. Pellegrino, D. Zanchet, C. Micheel, S.C. Williams, R. Boudreau, M.A.L. Gros, C.A. Larabell, A.P. Alivisatos, Biological applications of colloidal nanocrystals. *Nanotechnology* **14**(7), R15–R27 (2003). <https://doi.org/10.1088/0957-4484/14/7/201>
43. W.R. Algar, A.J. Tavares, U.J. Krull, Beyond labels: a review of the application of quantum dots as integrated components of assays, bioprobes, and biosensors utilizing optical transduction. *Anal. Chim. Acta* **673**(1), 1–25 (2010). <https://doi.org/10.1016/j.aca.2010.05.026>
44. J.F.F. Ribeiro, M.I.A. Pereira, L.G. Assis, P.E. Cabral Filho, B.S. Santos, G.A.L. Pereira, C.R. Chaves, G.S. Campos, S.I. Sardi, G. Pereira, A. Fontes, Quantum dots-based fluoroimmunoassay for anti-zika virus IgG antibodies detection. *J. Photochem. Photobiol. B* **194**, 135–139 (2019). <https://doi.org/10.1016/j.jphotobiol.2019.03.019>
45. Z. Deng, Y. Zhang, J. Yue, F. Tang, Q. Wei, Green and orange CdTe quantum dots as effective pH-sensitive fluorescent probes for dual simultaneous and independent detection of viruses. *J. Phys. Chem. B* **111**(41), 12024–12031 (2007). <https://doi.org/10.1021/jp074609z>
46. J.A. Berkenbrock, R. Grecco-Machado, S. Achenbach, Microfluidic devices for the detection of viruses: aspects of emergency fabrication during the COVID-19 pandemic and other outbreaks. *Proc. R. Soc. Math. Phys. Eng. Sci.* **476**(2243), 20200398 (2020). <https://doi.org/10.1098/rspa.2020.0398>
47. C. Tymm, J. Zhou, A. Tadimety, A. Burklund, J.X.J. Zhang, Scalable COVID-19 detection enabled by lab-on-chip biosensors. *Cell. Mol. Bioeng.* **13**(4), 313–329 (2020). <https://doi.org/10.1007/s12195-020-00642-z>
48. E. Nunez-Bajo, M. Kasimatis, Y. Cotur, T. Asfour, A. Collins, U. Tanriverdi, M. Grell, M. Kaisti, G. Senesi, K. Stevenson, F. Güder, Ultra-low-cost integrated silicon-based transducer for on-site, genetic detection of pathogens. bioRxiv, 2020.03.23.002931 (2020). <https://doi.org/10.1101/2020.03.23.002931>
49. R. Funari, K.-Y. Chu, A.Q. Shen, Detection of antibodies against SARS-CoV-2 spike protein by gold nanoparticles in an opto-microfluidic chip. *Biosens. Bioelectron.* **169**, 112578 (2020). <https://doi.org/10.1016/j.bios.2020.112578>
50. Q. Lin, D. Wen, J. Wu, L. Liu, W. Wu, X. Fang, J. Kong, Microfluidic immunoassays for sensitive and simultaneous detection of IgG/IgM/antigen of SARS-CoV-2 within 15 min. *Anal. Chem.* **92**(14), 9454–9458 (2020). <https://doi.org/10.1021/acs.analchem.0c01635>
51. A. Parihar, P. Ranjan, S.K. Sanghi, A.K. Srivastava, R. Khan, Point-of-care biosensor-based diagnosis of COVID-19 holds promise to combat current and future pandemics. *ACS Appl. Bio Mater.* **3**(11), 7326–7343 (2020). <https://doi.org/10.1021/acsabm.0c01083>
52. A. Basiri, A. Heidari, M.F. Nadi, M.T.P. Fallahy, S.S. Nezamabadi, M. Sedighi, A. Saghazadeh, N. Rezaei, Microfluidic devices for detection of RNA viruses. *Rev. Med. Virol.* **n/a**(n/a), e2154. <https://doi.org/10.1002/rmv.2154>
53. Z. Qin, R. Peng, I.K. Baravik, X. Liu, Fighting COVID-19: Integrated micro- and nanosystems for viral infection diagnostics. *Matter* **3**(3), 628–651 (2020). <https://doi.org/10.1016/j.matt.2020.06.015>
54. K.-S. Yun, D. Lee, H.-S. Kim, E. Yoon, A microfluidic chip for measurement of biomolecules using a microbead-based quantum dot fluorescence assay. *Meas. Sci. Technol.* **17**(12), 3178–3183 (2006). <https://doi.org/10.1088/0957-0233/17/12/S10>

55. J.M. Klostranec, Q. Xiang, G.A. Farcas, J.A. Lee, A. Rhee, E.I. Lafferty, S.D. Perrault, K.C. Kain, W.C.W. Chan, Convergence of quantum dot barcodes with microfluidics and signal processing for multiplexed high-throughput infectious disease diagnostics. *Nano Lett.* **7**(9), 2812–2818 (2007). <https://doi.org/10.1021/nl071415m>
56. J.V. Jokerst, A. Raamanathan, N. Christodoulides, P.N. Floriano, A.A. Pollard, G.W. Simmons, J. Wong, C. Gage, W.B. Furnaga, S.W. Redding, J.T. McDevitt, Nano-bio-chips for high performance multiplexed protein detection: determinations of cancer biomarkers in serum and saliva using quantum dot bioconjugate labels. *Biosens. Bioelectron.* **24**(12), 3622–3629 (2009). <https://doi.org/10.1016/j.bios.2009.05.026>
57. M. Hu, J. Yan, Y. He, H. Lu, L. Weng, S. Song, C. Fan, L. Wang, Ultrasensitive, multiplexed detection of cancer biomarkers directly in serum by using a quantum dot-based microfluidic protein chip. *ACS Nano* **4**(1), 488–494 (2010). <https://doi.org/10.1021/nn901404h>
58. H. Zhang, T. Xu, C.-W. Li, M. Yang, A microfluidic device with microbead array for sensitive virus detection and genotyping using quantum dots as fluorescence labels. *Biosens. Bioelectron.* **25**(11), 2402–2407 (2010). <https://doi.org/10.1016/j.bios.2010.02.032>
59. L. Chen, W.R. Algar, A.J. Tavares, U.J. Krull, Toward a solid-phase nucleic acid hybridization assay within microfluidic channels using immobilized quantum dots as donors in fluorescence resonance energy transfer. *Anal. Bioanal. Chem.* **399**(1), 133–141 (2011). <https://doi.org/10.1007/s00216-010-4309-0>
60. F. Long, C. Gu, A.Z. Gu, H. Shi, Quantum dot/carrier–protein/haptens conjugate as a detection nanobioprobe for FRET-based immunoassay of small analytes with all-fiber microfluidic biosensing platform. *Anal. Chem.* **84**(8), 3646–3653 (2012). <https://doi.org/10.1021/ac3000495>
61. H. Zhang, X. Hu, X. Fu, Aptamer-based microfluidic beads array sensor for simultaneous detection of multiple analytes employing multienzyme-linked nanoparticle amplification and quantum dots labels. *Biosens. Bioelectron.* **57**, 22–29 (2014). <https://doi.org/10.1016/j.bios.2014.01.054>
62. G. Kim, J.-H. Moon, C.-Y. Moh, J. Lim, A microfluidic nanobiosensor for the detection of pathogenic Salmonella. *Biosens. Bioelectron.* **67**, 243–247 (2015). <https://doi.org/10.1016/j.bios.2014.08.023>
63. L. Liang, M. Su, L. Li, F. Lan, G. Yang, S. Ge, J. Yu, X. Song, Aptamer-based fluorescent and visual biosensor for multiplexed monitoring of cancer cells in microfluidic paper-based analytical devices. *Sensors Actuators B Chem.* **229**, 347–354 (2016). <https://doi.org/10.1016/j.snb.2016.01.137>
64. X. Weng, S. Neethirajan, A microfluidic biosensor using graphene oxide and aptamer-functionalized quantum dots for peanut allergen detection. *Biosens. Bioelectron.* **85**, 649–656 (2016). <https://doi.org/10.1016/j.bios.2016.05.072>
65. B. Li, Z. Zhang, J. Qi, N. Zhou, S. Qin, J. Choo, L. Chen, Quantum dot-based molecularly imprinted polymers on three-dimensional origami paper microfluidic chip for fluorescence detection of phycocyanin. *ACS Sens.* **2**(2), 243–250 (2017). <https://doi.org/10.1021/acssensors.6b00664>
66. Y. Chen, X. Guo, W. Liu, L. Zhang, Paper-based fluorometric immunodevice with quantum-dot labeled antibodies for simultaneous detection of carcinoembryonic antigen and prostate specific antigen. *Microchim. Acta* **186**(2), 112 (2019). <https://doi.org/10.1007/s00604-019-3232-0>
67. L. Hao, L. Xue, F. Huang, G. Cai, W. Qi, M. Zhang, Q. Han, Z. Wang, J. Lin, A Microfluidic biosensor based on magnetic nanoparticle separation, quantum dots labeling and MnO₂ nanoflower amplification for rapid and sensitive detection of Salmonella Typhimurium. *Micromachines* **11**(3), 281 (2020). <https://doi.org/10.3390/mi11030281>
68. J. Zhou, B. Li, A. Qi, Y. Shi, J. Qi, H. Xu, L. Chen, ZnSe quantum dot based ion imprinting technology for fluorescence detecting cadmium and lead ions on a three-dimensional rotary paper-based microfluidic chip. *Sensors Actuators B Chem.* **305**, 127462 (2020). <https://doi.org/10.1016/j.snb.2019.127462>
69. Y. Wang, D. Zang, S. Ge, L. Ge, J. Yu, M. Yan, A novel microfluidic origami photoelectrochemical sensor based on CdTe quantum dots modified molecularly imprinted polymer and its highly selective detection of S-fenvalerate. *Electrochim. Acta* **107**, 147–154 (2013). <https://doi.org/10.1016/j.electacta.2013.05.154>
70. M. Medina-Sánchez, S. Miserere, E. Morales-Narváez, A. Merkoçi, On-chip magneto-immunoassay for Alzheimer's biomarker electrochemical detection by using quantum dots as labels. *Biosens. Bioelectron.* **54**, 279–284 (2014). <https://doi.org/10.1016/j.bios.2013.10.069>
71. A.S. Ghreera, C.M. Pandey, M.A. Ali, B.D. Malhotra, Quantum dot-based microfluidic biosensor for cancer detection. *Appl. Phys. Lett.* **106**(19), 193703 (2015). <https://doi.org/10.1063/1.4921203>
72. M. Medina-Sánchez, S. Miserere, M. Cadevall, A. Merkoçi, Enhanced detection of quantum dots labeled protein by simultaneous bismuth electrodeposition into microfluidic channel. *ELECTROPHORESIS* **37**(3), 432–437 (2016). <https://doi.org/10.1002/elps.201500288>
73. W. Ye, J. Guo, X. Bao, T. Chen, W. Weng, S. Chen, M. Yang, Rapid and sensitive detection of bacteria response to antibiotics using nanoporous membrane and graphene quantum dot (GQDs)-based electrochemical biosensors. *Materials* **10**(6), 603 (2017). <https://doi.org/10.3390/ma10060603>
74. C.T. Kokkinos, D.L. Giokas, A.S. Economou, P.S. Petrou, S.E. Kakabakos, Paper-based microfluidic device with integrated sputtered electrodes for stripping voltammetric determination of DNA via quantum dot labeling. *Anal. Chem.* **90**(2), 1092–1097 (2018). <https://doi.org/10.1021/acs.analchem.7b04274>
75. S. Wang, N. Mamedova, N.A. Kotov, W. Chen, J. Studer, Antigen/antibody immunocomplex from CdTe nanoparticle bioconjugates. *Nano Lett.* **2**(8), 817–822 (2002). <https://doi.org/10.1021/nl0255193>
76. R. Bakalova, Z. Zhelev, H. Ohba, Y. Baba, Quantum dot-based Western blot technology for ultrasensitive detection of tracer proteins. *J. Am. Chem. Soc.* **127**(26), 9328–9329 (2005). <https://doi.org/10.1021/ja0510055>
77. H. Yang, Q. Guo, R. He, D. Li, X. Zhang, C. Bao, H. Hu, D. Cui, A quick and parallel analytical method based on quantum dots labeling for ToRCH-related antibodies. *Nanoscale Res. Lett.* **4**(12), 1469–1474 (2009). <https://doi.org/10.1007/s11671-009-9422-7>
78. F. Wu, H. Yuan, C. Zhou, M. Mao, Q. Liu, H. Shen, Y. Cen, Z. Qin, L. Ma, L. Song Li, Multiplexed detection of influenza A virus subtype H5 and H9 via quantum dot-based immunoassay. *Biosens. Bioelectron.* **77**, 464–470 (2016). <https://doi.org/10.1016/j.bios.2015.10.002>
79. M. Park, H.D. Ha, Y.T. Kim, J.H. Jung, S.-H. Kim, D.H. Kim, T.S. Seo, Combination of a sample pretreatment microfluidic device with a photoluminescent graphene oxide quantum dot sensor for trace lead detection. *Anal. Chem.* **87**(21), 10969–10975 (2015). <https://doi.org/10.1021/acs.analchem.5b02907>
80. M. Park, T.S. Seo, An integrated microfluidic device with solid-phase extraction and graphene oxide quantum dot array for highly sensitive and multiplex detection of trace metal ions. *Biosens. Bioelectron.* **126**, 405–411 (2019). <https://doi.org/10.1016/j.bios.2018.11.010>
81. S. Panesar, X. Weng, S. Neethirajan, Toward point-of-care diagnostics of breast cancer: development of an optical biosensor using quantum dots. *IEEE Sens. Lett.* **1**(4), 1–4 (2017). <https://doi.org/10.1109/LSSENS.2017.2727983>

82. I.L. Medintz, A.R. Clapp, H. Mattoussi, E.R. Goldman, B. Fisher, J.M. Mauro, Self-assembled nanoscale biosensors based on quantum dot FRET donors. *Nat. Mater.* **2**(9), 630–638 (2003). <https://doi.org/10.1038/nmat961>
83. G. Crivat, S.M. Da Silva, D.R. Reyes, L.E. Locascio, M. Gaitan, N. Rosenzweig, Z. Rosenzweig, Quantum Dot FRET-based probes in thin films grown in microfluidic channels. *J. Am. Chem. Soc.* **132**(5), 1460–1461 (2010). <https://doi.org/10.1021/ja908784b>
84. W.R. Algar, D. Wegner, A.L. Huston, J.B. Blanco-Canosa, M.H. Stewart, A. Armstrong, P.E. Dawson, N. Hildebrandt, I.L. Medintz, Quantum dots as simultaneous acceptors and donors in time-gated Förster resonance energy transfer relays: characterization and biosensing. *J. Am. Chem. Soc.* **134**(3), 1876–1891 (2012). <https://doi.org/10.1021/ja210162f>
85. M. Chen, T.T. Nguyen, N. Varongchayakul, C. Gazon, M. Chern, R.C. Baer, S. Lecommandoux, C.M. Klapperich, J.E. Galagan, A.M. Dennis, M.W. Grinstaff, Surface immobilized nucleic acid–transcription factor quantum dots for biosensing. *Adv. Healthc. Mater.* **9**(17), 2000403 (2020). <https://doi.org/10.1002/adhm.202000403>
86. Z.S. Pehlivan, M. Torabfam, H. Kurt, C. Ow-Yang, N. Hildebrandt, M. Yüce, Aptamer and nanomaterial based fret biosensors: a review on recent advances (2014–2019). *Microchim. Acta* **186**(8), 563 (2019). <https://doi.org/10.1007/s00604-019-3659-3>
87. G. Annio, T.L. Jennings, O. Tagit, N. Hildebrandt, Sensitivity enhancement of Förster resonance energy transfer immunoassays by multiple antibody conjugation on quantum dots. *Bioconjug. Chem.* **29**(6), 2082–2089 (2018). <https://doi.org/10.1021/acs.bioconjchem.8b00296>
88. I. Vasilescu, S.A.V. Eremia, M. Kusko, A. Radoi, E. Vasile, G.-L. Radu, Molybdenum disulphide and graphene quantum dots as electrode modifiers for laccase biosensor. *Biosens. Bioelectron.* **75**, 232–237 (2016). <https://doi.org/10.1016/j.bios.2015.08.051>
89. Q. Liu, C. Ma, X.-P. Liu, Y.-P. Wei, C.-J. Mao, J.-J. Zhu, A Novel electrochemiluminescence biosensor for the detection of microRNAs based on a DNA functionalized nitrogen doped carbon quantum dots as signal enhancers. *Biosens. Bioelectron.* **92**, 273–279 (2017). <https://doi.org/10.1016/j.bios.2017.02.027>
90. J.A. Hansen, J. Wang, A.-N. Kawde, Y. Xiang, K.V. Gothelf, G. Collins, Quantum-dot/aptamer-based ultrasensitive multi-analyte electrochemical biosensor. *J. Am. Chem. Soc.* **128**(7), 2228–2229 (2006). <https://doi.org/10.1021/ja060005h>
91. F.H. Cincotto, E.L. Fava, F.C. Moraes, O. Fatibello-Filho, R.C. Faria, A new disposable microfluidic electrochemical paper-based device for the simultaneous determination of clinical biomarkers. *Talanta* **195**, 62–68 (2019). <https://doi.org/10.1016/j.talanta.2018.11.022>
92. J. Peng, S. Wang, P.-H. Zhang, L.-P. Jiang, J.-J. Shi, J.-J. Zhu, Fabrication of graphene quantum dots and hexagonal boron nitride nanocomposites for fluorescent cell imaging <https://www.ingentaconnect.com/content/asp/jbn/2013/00000009/00000010/art00003> (accessed May 6, 2020). <https://doi.org/10.1166/jbn.2013.1663>
93. Q. Zhang, F. Yang, S. Zhou, N. Bao, Z. Xu, M. Chaker, D. Ma, Broadband photocatalysts enabled by 0D/2D heterojunctions of near-infrared quantum dots/graphitic carbon nitride nanosheets. *Appl. Catal. B Environ.* **270**, 118879 (2020). <https://doi.org/10.1016/j.apcatb.2020.118879>
94. Y. Liu, K. Yan, J. Zhang, Graphitic carbon nitride sensitized with CdS quantum dots for visible-light-driven photoelectrochemical aptasensing of tetracycline. *ACS Appl. Mater. Interfaces* **8**(42), 28255–28264 (2016). <https://doi.org/10.1021/acsami.5b08275>
95. S. Lv, Y. Li, K. Zhang, Z. Lin, D. Tang, Carbon dots/g-C₃N₄ nanoheterostructures-based signal-generation tags for photoelectrochemical immunoassay of cancer biomarkers coupling with copper nanoclusters. *ACS Appl. Mater. Interfaces* **9**(44), 38336–38343 (2017). <https://doi.org/10.1021/acsami.7b13272>
96. Y.-X. Dong, J.-T. Cao, B. Wang, S.-H. Ma, Y.-M. Liu, Spatial-resolved photoelectrochemical biosensing array based on a CdS@g-C₃N₄ heterojunction: a universal immunosensing platform for accurate detection. *ACS Appl. Mater. Interfaces* **10**(4), 3723–3731 (2018). <https://doi.org/10.1021/acsami.7b13557>
97. D. Du, J. Ding, Y. Tao, H. Li, X. Chen, CdTe Nanocrystal-based electrochemical biosensor for the recognition of neutravidin by anodic stripping voltammetry at electrodeposited bismuth film. *Biosens. Bioelectron.* **24**(4), 863–868 (2008). <https://doi.org/10.1016/j.bios.2008.07.020>
98. H. Ji, F. Yan, J. Lei, H. Ju, Ultrasensitive electrochemical detection of nucleic acids by template enhanced hybridization followed with rolling circle amplification. *Anal. Chem.* **84**(16), 7166–7171 (2012). <https://doi.org/10.1021/ac3015356>
99. H. Dong, F. Yan, H. Ji, D.K.Y. Wong, H. Ju, Quantum-dot-functionalized poly (styrene-co-acrylic acid) microbeads: stepwise self-assembly, characterization, and applications for sub-femtomolar electrochemical detection of DNA hybridization. *Adv. Funct. Mater.* **20**(7), 1173–1179 (2010). <https://doi.org/10.1002/adfm.200901721>
100. J.-J. Zhang, T.-T. Zheng, F.-F. Cheng, J.-R. Zhang, J.-J. Zhu, Toward the early evaluation of therapeutic effects: an electrochemical platform for ultrasensitive detection of apoptotic cells. *Anal. Chem.* **83**(20), 7902–7909 (2011). <https://doi.org/10.1021/ac201804b>
101. L. Zheng, X. Li, P. Liu, G. Wu, X. Lu, X. Liu, Simultaneous detection of multiple DNA targets based on encoding metal ions. *Biosens. Bioelectron.* **52**, 354–359 (2014). <https://doi.org/10.1016/j.bios.2013.09.008>
102. S. Marin, A. Merkoçi, Direct electrochemical stripping detection of cystic-fibrosis-related DNA linked through cadmium sulfide quantum dots. *Nanotechnology* **20**(5), 055101 (2009). <https://doi.org/10.1088/0957-4484/20/5/055101>
103. J.A. Hansen, R. Mukhopadhyay, J.Ø. Hansen, K.V. Gothelf, Femtomolar electrochemical detection of DNA targets using metal sulfide nanoparticles. *J. Am. Chem. Soc.* **128**(12), 3860–3861 (2006). <https://doi.org/10.1021/ja0574116>
104. X. Li, J. Liu, S. Zhang, Electrochemical analysis of two analytes based on a dual-functional aptamer DNA sequence. *Chem. Commun.* **46**(4), 595–597 (2010). <https://doi.org/10.1039/B916304B>
105. C. Kokkinos, A. Economou, P.S. Petrou, S.E. Kakabakos, Microfabricated tin–film electrodes for protein and dna sensing based on stripping voltammetric detection of Cd(II) released from quantum dots labels. *Anal. Chem.* **85**(22), 10686–10691 (2013). <https://doi.org/10.1021/ac402783t>
106. C. Wang, J. Qian, K. An, X. Huang, L. Zhao, Q. Liu, N. Hao, K. Wang, Magneto-controlled aptasensor for simultaneous electrochemical detection of dual mycotoxins in maize using metal sulfide quantum dots coated silica as labels. *Biosens. Bioelectron.* **89**, 802–809 (2017). <https://doi.org/10.1016/j.bios.2016.10.010>
107. F.A. Esteve-Turrillas, A. Abad-Fuentes, Applications of quantum dots as probes in immunosensing of small-sized analytes. *Biosens. Bioelectron.* **41**, 12–29 (2013). <https://doi.org/10.1016/j.bios.2012.09.025>
108. E.L. Fava, T.A. Silva, T.M. do Prado, F.C. de Moraes, R.C. Faria, O. Fatibello-Filho, Electrochemical paper-based microfluidic device for high throughput multiplexed analysis. *Talanta* **203**, 280–286 (2019). <https://doi.org/10.1016/j.talanta.2019.05.081>
109. D. Evans, K.I. Papadimitriou, N. Vasilakis, P. Pantelidis, P. Kelleher, H. Morgan, T. Prodromakis, A Novel microfluidic point-of-care biosensor system on printed circuit board for

- cytokine detection. *Sensors* **18**(11), 4011 (2018). <https://doi.org/10.3390/s18114011>
110. Y. Piao, X. Wang, H. Xia, W. Wang, Digital microfluidic platform for automated detection of human chorionic gonadotropin. *Microfluid. Nanofluid.* **23**(1), 1 (2018). <https://doi.org/10.1007/s10404-018-2168-8>
 111. L.J. Lucas, J.N. Chesler, J.-Y. Yoon, Lab-on-a-chip immunoassay for multiple antibodies using microsphere light scattering and quantum dot emission. *Biosens. Bioelectron.* **23**(5), 675–681 (2007). <https://doi.org/10.1016/j.bios.2007.08.004>
 112. S. Wang, L. Zheng, G. Cai, N. Liu, M. Liao, Y. Li, X. Zhang, J. Lin, A microfluidic biosensor for online and sensitive detection of *Salmonella typhimurium* using fluorescence labeling and smartphone video processing. *Biosens. Bioelectron.* **140**, 111333 (2019). <https://doi.org/10.1016/j.bios.2019.111333>
 113. J.-W. Choi, W.K. Oh, H.J. Thomas, R.W. Heineman, H. Brian Halsall, H.J. Nevin, J.A. Helmicki, H. Thurman Henderson, H.C. Ahn, An integrated microfluidic biochemical detection system for protein analysis with magnetic bead-based sampling capabilities. *Lab Chip* **2**(1), 27–30 (2002). <https://doi.org/10.1039/B107540N>
 114. L. Reverté, B. Prieto-Simón, M. Campàs, New advances in electrochemical biosensors for the detection of toxins: nanomaterials, magnetic beads and microfluidics systems. A review. *Anal. Chim. Acta* **908**, 8–21 (2016). <https://doi.org/10.1016/j.aca.2015.11.050>
 115. V.N. Goral, V.N. Zaytseva, J.A. Baeumner, Electrochemical microfluidic biosensor for the detection of nucleic acid sequences. *Lab Chip* **6**(3), 414–421 (2006). <https://doi.org/10.1039/B513239H>
 116. S.-E. Kim, M.V. Tieu, S.Y. Hwang, M.-H. Lee, Magnetic particles: their applications from sample preparations to biosensing platforms. *Micromachines* **11**(3), 302 (2020). <https://doi.org/10.3390/mi11030302>
 117. T. Songjaroen, W. Dungchai, O. Chailapakul, W. Laiwattanapaisal, Novel, Simple and low-cost alternative method for fabrication of paper-based microfluidics by wax dipping. *Talanta* **85**(5), 2587–2593 (2011). <https://doi.org/10.1016/j.talanta.2011.08.024>
 118. C. Carrell, A. Kava, M. Nguyen, R. Menger, Z. Munshi, Z. Call, M. Nussbaum, C. Henry, Beyond the lateral flow assay: a review of paper-based microfluidics. *Microelectron. Eng.* **206**, 45–54 (2019). <https://doi.org/10.1016/j.mee.2018.12.002>
 119. A. Nilghaz, L. Guan, W. Tan, W. Shen, Advances of paper-based microfluidics for diagnostics—the original motivation and current status. *ACS Sens.* **1**(12), 1382–1393 (2016). <https://doi.org/10.1021/acssensors.6b00578>
 120. B. Li, W. Zhang, L. Chen, B. Lin, A fast and low-cost spray method for prototyping and depositing surface-enhanced Raman scattering arrays on microfluidic paper based device. *ELECTROPHORESIS* **34**(15), 2162–2168 (2013). <https://doi.org/10.1002/elps.201300138>
 121. Q. Kong, Y. Wang, L. Zhang, S. Ge, J. Yu, A novel microfluidic paper-based colorimetric sensor based on molecularly imprinted polymer membranes for highly selective and sensitive detection of bisphenol A. *Sensors Actuators B Chem.* **243**, 130–136 (2017). <https://doi.org/10.1016/j.snb.2016.11.146>
 122. E. Carrilho, A.W. Martinez, G.M. Whitesides, Understanding wax printing: a simple micropatterning process for paper-based microfluidics. *Anal. Chem.* **81**(16), 7091–7095 (2009). <https://doi.org/10.1021/ac901071p>
 123. M. Sher, R. Zhuang, U. Demirci, W. Asghar, Paper-based analytical devices for clinical diagnosis: recent advances in the fabrication techniques and sensing mechanisms. *Expert. Rev. Mol. Diagn.* **17**(4), 351–366 (2017). <https://doi.org/10.1080/14737159.2017.1285228>